AD-A118 234 TRINITY COLL DUBLIN (IRELAND) DEPT OF CIVIL ENGINEERING F/G 20/11
NUMERICAL METHODS FOR CREEP ANALYSIS IN GEOTECHNICAL PROBLEMS.(U)
DEC 81 T E GLYNN DAERO-76-G-063
UNCLASSIFIED NL

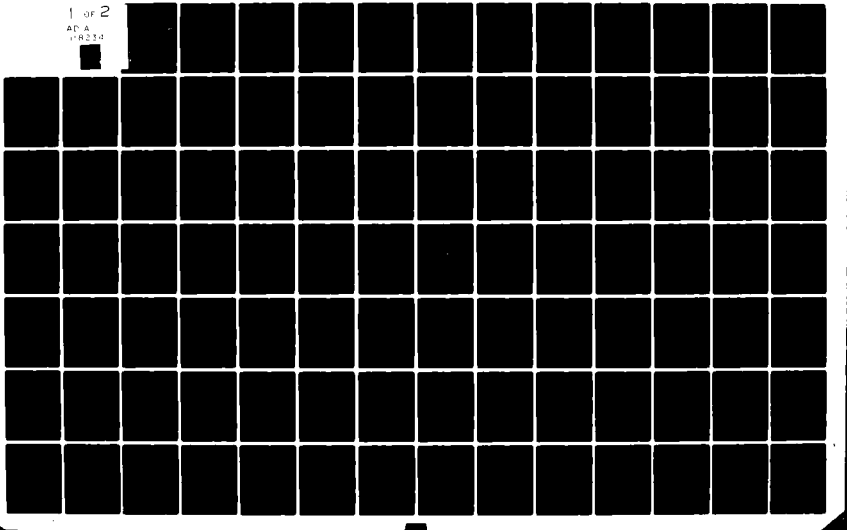

(12)

NUMERICAL METHODS FOR CREEP ANALYSIS IN GEOTECHNICAL PROBLEMS

FINAL TECHNICAL REPORT

by

T. E. GLYNN

Civil Engineering
Department
Trinity College

To

EUROPEAN RESEARCH OFFICE
United States Army

GRANTEE

UNIVERSITY OF DUBLIN
ENGINEERING SCHOOL
TRINITY COLLEGE

GRANT NO. DAERO - 76 - G - 063
December 1981.

Project Title PAVEMENT RESEARCH

Report Title

NUMERICAL METHODS FOR CREEP ANALYSIS IN GEOTECHNICAL PROBLEMS

FINAL TECHNICAL REPORT

BY

T.E. GLYNN

DEPARTMENT OF CIVIL ENGINEERING
TRINITY COLLEGE

Grantee

University of Dublin
Engineering School
Trinity College
Dublin.

The research reported in this document has been made possible through the support and sponsorship of the United States Army through its European Research Office.

SYNOPSIS

This report presents the results of a theoretical study of inelastic material behaviour produced by static loading on a viscous continuum. A number of issues are addressed in an attempt to introduce inelastic behaviour into piecewise numerical methods. Methods based on similitude and direct integration of the displacement field are investigated. Potential field theory is invoked as a means of describing stress distributions which are assumed invariant with respect to time of straining the material. No attempt has been made to include forced flow, strain hardening or frictional material properties. The analysis is restricted to slow deformations and results in a line integral for conversion of strain rate to displacement as a function of time of straining. The interpretation of experimental data is viewed from the stand-point of functional analysis as it is felt that this branch of mathematics has unexplored implications in the study of creep of deformable bodies.

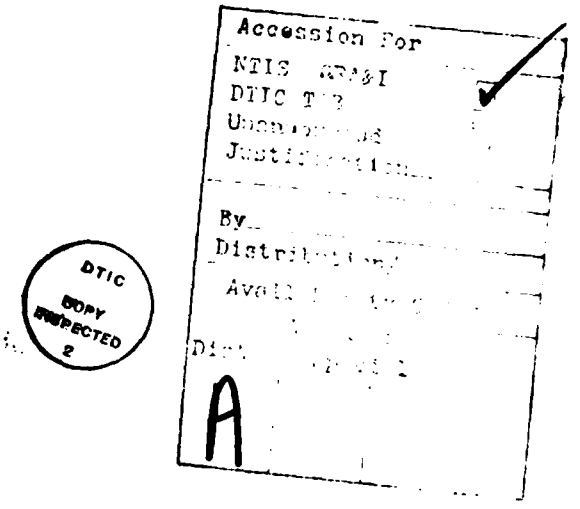

ACKNOWLEDGEMENTS

The author gratefully acknowledges the sponsorship of the U.S. Army through its European Research Office. Personal thanks is extended to the former chief scientist of E.R.O. Dr. Hoyt Lemons and to the present chief scientist Warren E. Grabau for their guidance and co-operation.
The encouragement afforded by Professor W. Wright, Head of the Engineering School, to conduct fundamental research is appreciated.
Assistance with closed form solutions and reference sources given by mathematician Victor Graham is gratefully acknowledged.
Thanks to Professor J.G.Byrne, Head of the Computer Science Department, for facilitating development of computer programs.
Programming assistance was provided by Mrs. Rosemary Welsh and by Gary Lyons who also draughted the diagrams in the report.

TABLE OF CONTENTS

CHAPTER 1

Theoretical Background of Creep Analysis

1.1 *Introduction*

This report covers the period from August 1976 to December 1981 for research under Grant No. DA ERO-76-G-063. The object of the research stipulated in the grant documentation was to compliment earlier experimental study of flexible pavements by fundamental analysis of materials under stress. The main objective is to find solutions for unrestrained flow such as the rutting of flexible payments and settlement of structures. The original proposal was accepted 6 August 1976 and subsequently was the subject of one modification designated DRXSN-E-AO, of March 1977.

This report presents the results of a theoretical study of inelastic material behaviour in a stress field produced by static loading of a viscous continuum. During the course of the project it transpired that the original objectives became somewhat eclipsed by theoretical development of wider scope. Procedures which employ the mathematical background of continuum mechanics to the solution of the longstanding engineering problem of slow creep of materials are described. While the theme of application to highway engineering underscores the study in this report the development of ideas is generalised to encompass a variety of problems in geotechnical engineering. No attempt has been made to confine the study to specific materials, but for the sake of some simplification the discussion of certain types of inelastic bahaviour have been omitted e.g. flow of granular materials, strain hardening substances.

A number of issues are addressed in an attempt to introduce inelastic behaviour into piecewise numerical construction of solutions of some generality in the mechanics of solids. The project commenced with a review of existing theory and solution methods to be found in the extensive literature on creep and plastic flow. The author's previous experience of unresolved problems in geotechnical engineering provided motives and guidance to the ultimate requirements of further theoretical development. The text will demonstrate that no definitive line is taken in the preparation of this report: rather the problem is attacked from a number of standpoints in a search for common ground of a unified theory; the problem is treated at different levels of complexity, but generally the aim is simplification of existing analytical methods.

These methods comprise classical plasticity which exhibits path dependent but time independent behaviour; classical viscoelasticity and creep theory both of which have path dependent and time dependent components. To avoid infringing on the technical meaning of viscoelastic and plastic behaviour the theoretical developments herein may be described as that which applies to material in the mastic state e.g. asphalt or remoulded clay. A brief statement of the classical theories follows.

Plasticity The task of plastic theory is twofold: first to set up relationships between stress and strain which describes adequately the observed plastic deformation of the material in laboratory tests, and second to

develop techniques for using these relationships in analysis and design. At least two variants of the theory are in common usage - the ideal rigid plastic and the elastoplastic models. These models employ the concepts of yield surface, associated flow rules and plastic potential functions. Throughout the theory time enters as a dummy variable only, while stresses and deformations are viewed as incremental rather than total entities. There is just one expression in plasticity theory that conceivably has a bearing on the creep problem, i.e. the expression for strain in terms of plastic potential viz.

$$\frac{d\varepsilon_i}{dt} = \lambda \frac{\delta f}{\delta \sigma_i} \qquad i = 1 \ldots 3 \qquad 1.1$$

where f denotes a yield function

" σ denotes stress.

The theory poses the problem that for real materials it requires considerable experimental work to define the yield function $f(\sigma)$.

Viscoelasticity The theory of linear viscoelasticity is well established and may be summarised in the set of expressions, Adeyeriand Krizek (1969):

Relaxation law

$$S_{ij}(x,t) = \int_{-\alpha}^{t} G_1(t-\tau) \frac{\delta e_{ij}(x,\tau)}{\delta \tau} d\tau$$

$$\sigma_{kk}(x,t) = \int_{-\alpha}^{t} G_2(t-\tau) \frac{\delta \varepsilon_{kk}(x,t)}{\delta \tau} d\tau$$

Creep law

$$e_{ij}(x,t) = \int_{-\alpha}^{t} J_1(t-\tau) \frac{\delta S_{ij}(x,\tau)}{\delta \tau} \, d\tau$$

$$\varepsilon_{kk}(x,t) = \int_{-\alpha}^{t} J_2(t-\tau) \frac{\delta \sigma_{kk}(x,\tau)}{\delta \tau} \, d\tau \qquad 1.2$$

where G and J denote relaxation moduli and creep compliances respectively,

S_{ij} denotes the deviatoric stress tensor

ε_{ij} " the strain tensor

e_{ij} " the deviatoric strain tensor

$x = (x_1, x_2, x_3)$ is a fixed Cartesian co-ordinate system.

The theory is based on the premise that stress depends principally on the rate at which the material is deformed according to the rheological relationship

$$\sigma_i = E\varepsilon_i + \eta \frac{d\varepsilon_i}{dt} \qquad i = 1 \ldots 3$$

where E denotes Young's modulus

η is the viscous coefficient

The theory is particularly applicable to problems of forced flow where boundary stresses are clearly a function of the rate of deformation - as for instance extrusion of a tube of toothpaste. In free flow problems the theory is less satisfactory as in certain cases it predicts deformation that tends to unrelasitic values as the time scale is extended. This feature appears in the application of viscoelasticity to rutting of flexible pavements, Thrower (1977).

Viso-plasticity This theory aims at generalisation

of viscous and plastic deformation on the assumption that the material behaves as an elastic solid exhibiting a zero rate of straining for stresses which are below a threshold or yield value. When the threshold stress is exceeded, flow begins at a rate which is a function of the excess stress.

The strain rate is related to the yield function in the form, Zienkiewicz and Godbole (1975)

$$\frac{d\varepsilon_i}{dt} = \frac{1}{\bar{\mu}} < F^n > \frac{\delta F}{\delta \sigma_i} \qquad 1.3$$

where $\bar{\mu}$ is some viscous parameter and $F(\sigma)$ represents the yield function,

Hence the notation

$$< F > = 0 \quad \text{if} \quad F < 0$$
$$< F > = F \quad \text{if} \quad F > 0$$

The resemblance between equations 1.1 and 1.3 is obvious and for $\bar{\mu} = 0$ the visco-plastic and ideal plastic formulations yield identical results.

Theory of Creep The various formulations of the theory of creep are collected in the works of Penny and Marriott (1971), Rabotnov (1953), Arutyunyan (1966) and several other authors. The treatise due to N. Kh. Arutyunyan is of particular interest because for the most part it deals with analyses of unrestrained creep flow in civil engineering applications. The advanced mathematical treatment undertaken for the creep of

concrete structures serves to highlight the complexity of closed form analysis. However his analysis discloses very practical results which are stated in the form of theorems thusly:

Theorem 1: If the stress condition of a given body is produced by the action of external forces, and its creep function for uniaxial stress $C(t,\tau)$ is proportional, with constant coefficient of proportionality k_o to the creep function for pure shear $w(t,\tau)$ then the system of stresses in the body considered coincides identically with the system of stresses of the corresponding instantaneous elastic problem.

Theorem 2: If the stress condition in a body either is constant or changes linearly with the x,y,z coordinates then the stresses in the body during creep will coincide with the stresses of the corresponding instantaneous elastic problem for the same body with different coefficients of lateral compression

$$v_1(t) \text{ and } v_2(t,\tau)$$

The theorems are the outcome of the following assumptions:

1. The material is regarded as a homogeneous isotropic body;
2. The relationship between creep deformation and stresses is linear;
3. The law of superposition applies to creep deformation.
4. The functions that characterize the changes in the coefficient of lateral compression for elastic deformation and creep deformation are identical, i.e. $v_1(\tau) = v_2(t,\tau) = v$.

The theorems are interpreted to mean that for unrestrained slow creeping flow of a material the stress distribution is not significantly different from that of the elasticity analysis for steady state boundary stresses. Of course if the boundary conditions permit a relaxation of stress anywhere in the domain then the stress distribution will adjust itself to minimise stress concentration as is the case with forced flow.

The approach of Arutyunyan is essentially that of the hereditary integral method which originated with Boltzmann and was further developed in the works of Volterra. The fundamental expressions of the theory in Arutyunyan's notation (see page 10 of his book) reads as follows:

$$\varepsilon_x(t) = \frac{\sigma_x(t)\left[1+v_1(t)\right]-v_1(t)(S(t)}{E(t)}$$

$$- \int_{\tau_1}^{t} \{\sigma_x(\tau)\frac{\delta}{\delta\tau}|\delta(t,\tau)+\delta_1(t,\tau)|-S(\tau)\ \frac{\delta\delta_1(t,\tau)}{\delta\tau}\}d\tau$$

$$\gamma_{xy} = 2\left\{\frac{\left[1+v_1(t)\right]\tau_{xy}(t)}{E(t)}\right.$$

$$\left. - \int_{\tau_1}^{t} \tau_{xy}(\tau)\frac{\delta}{\delta\tau}|\delta(t,\tau)+\delta_1(t,\tau)|d\tau\right\}$$

$$\rightarrow (x,y,z) \qquad 1.4$$

where

$$\delta(t,\tau) = \frac{1}{E(\tau)} + C(t,\tau);$$

$$\delta_1(t,\tau) = \frac{v_1(\tau)}{E(\tau)} + v_2(t,\tau)C(t,\tau);$$

$$S(t) = \sigma_x(t) + \sigma_y(t) + \sigma_z(t)$$

Remaining relations obtained by cyclic permutation of x,y,z. In above formulae all the stress components begin to act simultaneously at time $\tau = \tau_1$. These basic equations of the hereditary integral method describe the process of deformation in a body by taking into account the changes of both its volume and its shape.

The difficulty in the construction of a theory of creep by this approach consists in the choice of the kernels in the integral equations on the basis of which solutions may be obtained for the fundamental problems of equilibrium of a creep-elastic medium.

Arutyunyan extended the linear theory to non-linear creep where the constitutive relationships do not entail linearity between stress and creep deformation at specific times. He found that the governing differential equation is the generalised Riccati equation on the assumption that the stress-strain-time relationship is only slightly non linear. The problem of non-linear creep was found to reduce to the solution of an equation of the form:

$$\frac{d^2u}{dt^2} + a\frac{du}{dt} = bE_o u(t)\left[E'(t) + y\varepsilon(t)\right]$$

where $\sigma(t) = \frac{u'(t)}{ub}$ and the remaining notation is defined in the original text pp. 264-267.

1.2 *Problem Statement*

The foregoing review of theory serves to illustrate the complex nature of any attempt at a closed form solution of material flow under stress. The formulation of constitutive stress-strain relations presents a formidable challenge and to incorporate these in a boundary value problem is even more exacting. Consequently simplified numerical schemes is a desirable goal. The fact that the geometrical configuration is not the prime source of difficulties suggests that an analysis developed for a particular geometry may be readily extendable to other configurations. In this work the author will concentrate on so-called axisymmetric flow problems with the conviction that the development could equally apply to plane strain or plane stress problems albeit with some modification to the analyses. The axisymmetric case is of common occurrence in foundation engineering as for instance a circular storage tank on soft ground, wheel loads on an asphalt pavement or a circular cofferdam on a compressible stratum.

The boundary value problem resembles the classical Boussinesq problem - that of a concentrated or distributed load on the surface of a semi-infinite half-space. The thrust of the analysis will be to develop a numerical technique for estimating the displacements beneath a flexible uniformly loaded circular contact area located on the free boundary of a semi-infinite half space of homogeneous mastic material. The analysis will delve into flow of thick cylinders subjected to radial forcing pressures (internal and external).

The task of developing the numerical procedure consists of the following steps:

i. postulate a mechanism of flow i.e. establish the geometry of a plausible mode of flow deformation.

ii. for an incremented flow of this mechanism integrate the work dissipated in non-recoverable deformation over the whole domain (or a part thereof).

iii. equate the energy supplied by the forcing pressure to the internal work and hence find the displacement at the source of the disturbing force as a function of elapsed time of loading.

iv. investigate method of substituting unprocessed test data for constitutive relationships in the analysis.

This scheme constitutes the direct method of solution and undoubtedly presents a number of obstacles, but it is in the spirit of finite element analysis. The main difficulty is that of specifying the constitutive relations for deformation in mutually perpendicular frames of reference i.e. creep laws in terms of stress invariants. On the other hand an indirect method based on similitude offers an alternative scheme. The application of similitude and dimensional analysis is known to produce practical solutions to otherwise intractable problems, Glen Murphy (1953). Both possibilities will be investigated in this report.

CHAPTER 2

A METHOD OF CALCULATING TIME-DEPENDENT DEFORMATION

2.1 *Introduction*

A draw-back to the methods outlined in Chapter 1 is the necessity to idealise the response of real materials to such an extent that the stress-strain relationship fits into the scheme of a particular theory. The constitutive equations tend to reflect the type of proposed analysis rather than actual behaviour i.e. rheological models for viscoelasticity and flow rules for plasticity. Whereas the real behaviour may reflect a variety of responses, the classical theories deal with preselected components. This approach results in a proliferation of material parameters, constants and exponents in the effort to fit experimental data. In what follows the author proposes an alternative method for the special case of axisymmetric flow under the action of sustained loading. The basic idea is to relate the flow problem to an experimental investigation of a corresponding model of the stress state using the minimum of data processing of the test results. In principle the method should prove equally valid for both linear and non-linear behaviour provided the stress state can be simulated in the test procedure. To fix ideas we consider only axisymmetric flow in non-forced boundary value problems; such processes of flow as metal forming with dies or presses are excluded at this stage in the development of the theory.

Initially theoretical aspects are explored, one of which is presented in this Chapter. The theoretical exercises are merely the forerunners to the main thrust of the work, namely the preparation of a scheme for numerical analysis by computer.

2.2 *Theoretical Considerations*

The time-dependent behaviour under consideration is a slow process commonly known as creep. Because inertial effects are excluded the laws of statics are applicable in the set of equipibrium equations of elasticity theory. For the purpose of this analysis it is appropriate to consider the equilibrium equations with respect to curvilinear coordinates. Curvilinear coordinates must be considered as being embedded in the material and are defined in terms of a function which is assigned some value at each point throughout the material. The direction and curvature of the coordinates therefore changes from point to point. Let the first family of curves be defined by

$$f(x,y) = \alpha$$

and the second family be defined by

$$g(x,y) = \beta$$

where x and y are rectangular coordinate components. For the case of a two-dimensional stress state referred to curvilinear coordinates the equilibrium equations are given by the expressions, Ford and Alexander (1976):

$$\frac{\delta\sigma_\alpha}{\delta\alpha} + \frac{\delta\zeta_{\alpha\beta}}{\delta\beta} + \frac{\sigma_\alpha - \sigma_\beta}{\rho_\beta} - \frac{2\zeta_{\alpha\beta}}{\rho_\alpha} = 0 \qquad \text{(a)}$$

$$\frac{\delta\sigma_\beta}{\delta\beta} + \frac{\delta\zeta_{\beta\alpha}}{\delta\alpha} - \frac{\sigma_\beta - \sigma_\alpha}{\rho_\alpha} + \frac{2\zeta_{\beta\alpha}}{\rho_\beta} = 0 \qquad \text{(b)} \qquad (2.1)$$

Where ρ_α and ρ_β denote radii of curvature, and σ and τ are direct and shearing stresses, respectively.

If the coordinate axes are chosen to coincide with the directions of principal velocity components, then for materials that exhibit sliding on planes inclined at 45 degrees to the principal planes, the equations of equilibrium in two dimensions along lines of maximum shear stress can be written in the form, Kuske and Robertson (1974)

$$\frac{\delta(\sigma_1+\sigma_2)}{\delta\alpha} - \frac{\delta(\sigma_1-\sigma_2)}{\delta\beta} - \frac{2(\sigma_1-\sigma_2)}{\rho_2} = 0 \qquad \text{(a)}$$

$$\frac{\delta(\sigma_1+\sigma_2)}{\delta\beta} - \frac{\delta(\sigma_1-\sigma_2)}{\delta\alpha} + \frac{2(\sigma_1-\sigma_2)}{\rho_1} = 0 \qquad \text{(b)}$$

2.2

where σ_1, σ_2 are the principal stresses at the point and ρ_1, ρ_2 denote the radii of curvature of the lines of maximum shear

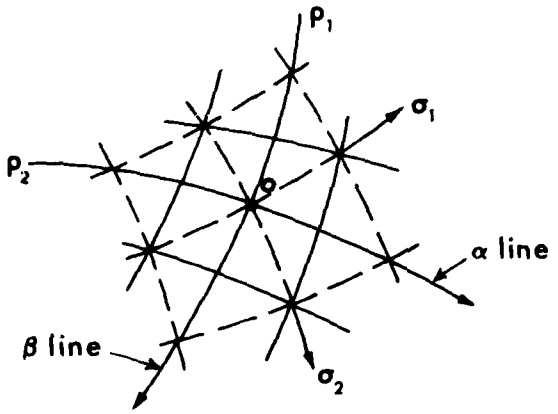

FIG. 2.1: *Element Bounded by Lines of Maximum Shear Stress*

Equation 2.2 provides the equilibrium conditions for the state of stress shown in Fig. 2.1. This state consists of the distributions of the mean normal stress and shears along the trajectories of the curvilinear coordinate system. The stresses at any point within a cell reduce to the mean normal stress and the maximum shear stresses. If we confine the analysis herein to materials that flow along planes of maximum shear stress the net is geometrically an orthogonal mesh. Materials that possess a Coulomb frictional component are thus excluded. In the notation of the slip-line theory of plasticity the geometry is termed an α,β net. The α,β lines can be assigned curvilinear coordinate values according to scale of plot but one of the lines - the β line - has the physical significance that it is the contour of constant normal stress. The β - lines are readily determined as the contours of mean stress for boundary value problems by solution of Laplace's equation viz.

$$\left(\frac{\delta^2}{\delta\alpha^2} + \frac{\delta^2}{\delta\beta^2}\right)(\sigma_\alpha+\sigma_\beta) \rightarrow \left(\frac{\delta^2}{\delta x^2} + \frac{\delta^2}{\delta y^2}\right)(\sigma_x+\sigma_y) = 0 \qquad 2.3$$

which follows from the invariance of the Laplacian under transformation of coordinate axes. The equation 2.3 provides the basis for the photoelastic technique because it implies that stress distribution is independent of the elastic constants of a homogeneous medium. The

conjugate function gives the velocity characteristics α - lines*. It would be a simple matter to plot the locations of the α - lines if the shear stress component could be used as an argument of Laplace's equation, but since this is not the case harmonic analysis only partially solves the problem of plotting the slip-line field. The method of stream functions has been used to find the geometry of the α - lines separately from the β - lines by many investigators in the field of fluid mechanics. In Chapter 5 of this report, a method of locating the α - lines is presented.

---

* The term velocity characteristic is borrowed from plasticity theory notwithstanding the fact that the governing equation 2.3 is elliptic.

2.3 *A Theory of Flow based on Stress Gradient*

Consider two-dimensional stress state with reference to curvilinear coordinates as depicted in Fig. 2.2. Inspection of the Equations 2.1 & 2.2 reveals that the source of viscous flow is the activation produced by the first term, namely, the gradient of the mean stress normal to the direction of flow, i.e. the mean normal stress variation along α - lines of Fig. 2.2.

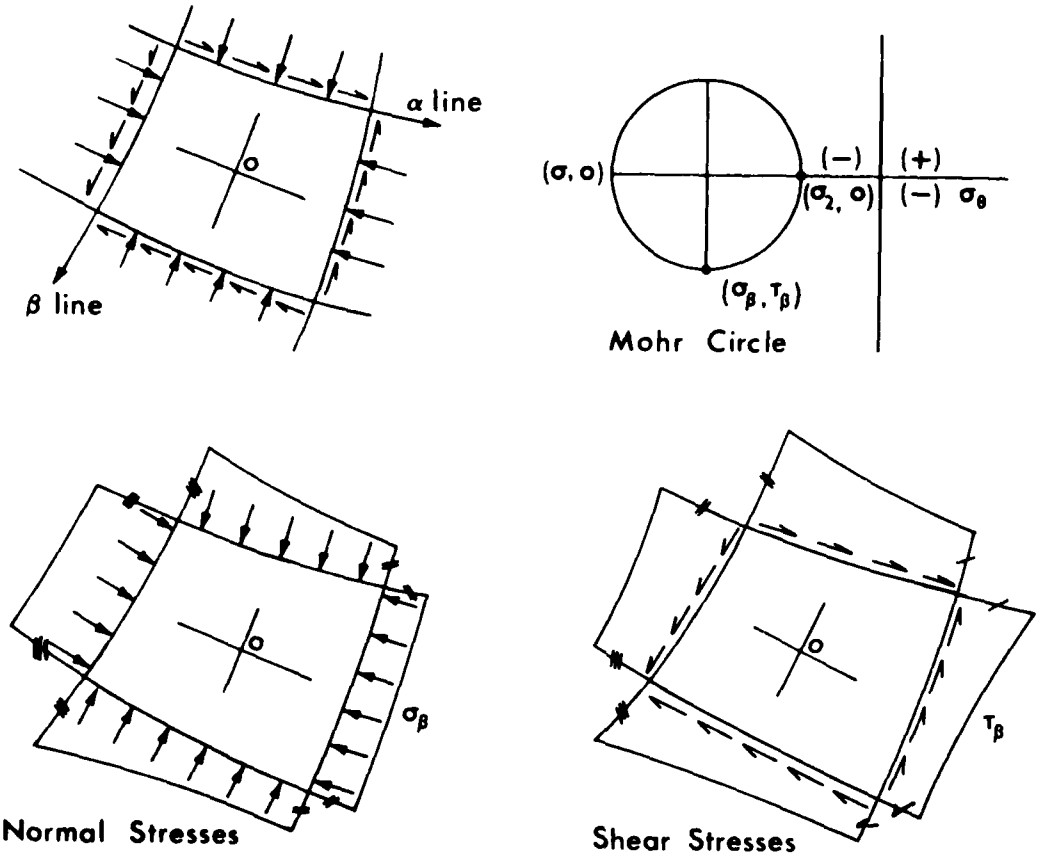

FIG. 2.2: *Stress Distribution in Cell of the* α-β *Net*

Equilibrium is preserved by the shear stress distribution on intersecting trajectories as shown by the remaining terms in the equations. In particular for large radii of curvature of the trajectories the third term of Equation 2.2 makes only a small contribution to equilibrium. Now in a viscous continuum the shearing stresses are not able to completely restrain permanent deformation once the material has absorbed the elastic strain energy of the stress state. Thus the phenomenon of creep ensues or for certain boundary conditions a relaxation of stress occurs.

The stress gradient along a flow path bounded by two α - lines is induced by the boundary traction because the source is the external pressure on the zone bounded by the same α - lines. The task is to relate the creep in a model test to the stress gradient in the test and subsequently to use the correlation for the purpose of predicting flow in a prototype of the boundary value problem. To accomplish the transition from model to prototype it is essential that a unique expression of the stress gradient be found. If the material behaviour is linear the so-called unique expression need only be determined for a single value of the stress state, but for non-linear material a relationship over a range of values of stress presumably is required. Such a unique relationship will advance the theory to the extent that it provides the link between driving forces in model and prototype.

In the search for a unique correlating function the author was attracted to the properties of the Laplace transform. It is well known that the transform confers the capability of distinguishing between functions which produce the same value for their integrals over some one interval. By definition we have the Laplace transform with independent parameter p.

$$L\{f(x)\} = \int_{x=o}^{\infty} f(x)e^{-px}dx \qquad 2.4$$

Clearly it is not appropriate to assign values to p if we are searching for a unique expression in the hope that a function such as the distribution of stress gradient can be characterised by a single numerical value. These considerations have led to the introduction of a special function which bears resemblance to Laplace transformation formulae; it has the same property - that of attenuating the function towards the end of its domain. The proposed function has the form $e^{-\frac{x-a}{b-x}}$ which replaces e^{-px} of the Laplace transform. By analogy we can write for a flow path the unique expression for distribution of $f(x)$ as follows:

$$G\{f(x)\} = \int_{\eta}^{[a,b]} f(x)e^{-\frac{x-a}{b-x}}dx \qquad 2.5$$

where a and b are the extremal points of path η.

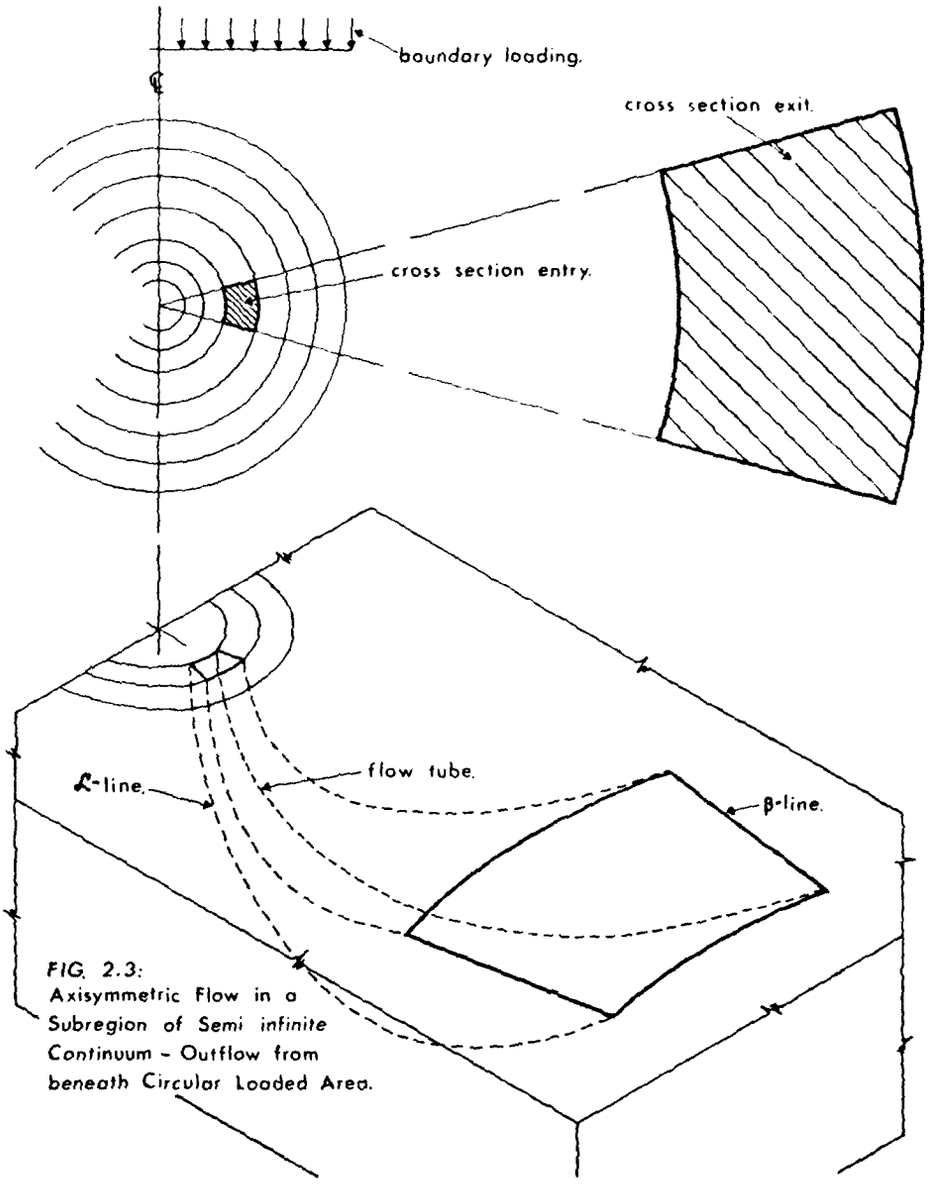

FIG. 2.3:
Axisymmetric Flow in a Subregion of Semi infinite Continuum – Outflow from beneath Circular Loaded Area.

The correspondence between prototype and model can now be postulated by assuming that for equal values of G and the same area subjected to surface traction the power expended in producing permanent deformation is identical; and where the G function is different for prototype and model the boundary velocities for the prototype follow from similitude according to the relationship:

$$v_p = \frac{G_p \sigma_p}{G_m \sigma_m} \times v_m \qquad 2.6$$

where σ denotes the driving stress on the boundary

v denotes velocity at the source

and subscripts p and m mean prototype and model, respectively.

To illustrate the physical meaning of Equation 2.6 we take for our model the radial flow in the wall of a thick cylinder under internal pressure and for the prototype the axially symmetric deformation of a semi-infinite viscous continum subjected to uniform pressure on a circular contact area as shown in Fig. 2.3. To achieve a correspondence we must compare the G-values on paths that have corresponding stress states. Firstly consider the case of linear material behaviour. An expansion test on a thick cylinder will provide the information to solve Equation 2.6 because the only unknown quantity is the velocity (v_p); the velocity will in general be a function of time and hence displacements will need to be determined by integration over an interval of time or alternatively as a set of Riemann sums. Second for non-linear materials the only

departure from the procedures outlined above is that the relationship between the velocity and the transform G be determined by test on a suitable model of the stress state over a range of the stresses. The whole process is considerably simplified if the assumption of incompressibility of the material is tenable. For many materials susceptible to creep this is approximately true once the elastic deformations have developed. The term $e^{-\frac{x-a}{b-x}}$ in the closed interval (a,b) produces the decay expression with numerical values as follows:-

$\frac{x-a}{b-x}$	$e^{-\frac{x-a}{b-x}}$
0	1.0000
0.2	0.8187
0.4	0.6703
0.6	0.5488
0.8	0.4493
1.0	0.3679
2.0	0.1353
4.0	0.0183
6.0	0.0025
8.0	0.0003
10.0	0.00005

The scheme can now be applied to our problem as depicted in Fig. 2.4. The velocity field is taken along a line midway between two α - lines which gives the path of integration of the function $G\{\sigma'_\beta(\alpha)\}$ where $\sigma'_\beta(\alpha)$ is the <u>gradient</u> of the normal stress in the α-direction. The forcing function is simply the boundary pressure multiplied by the area of the flow 'tube' at the boundary.

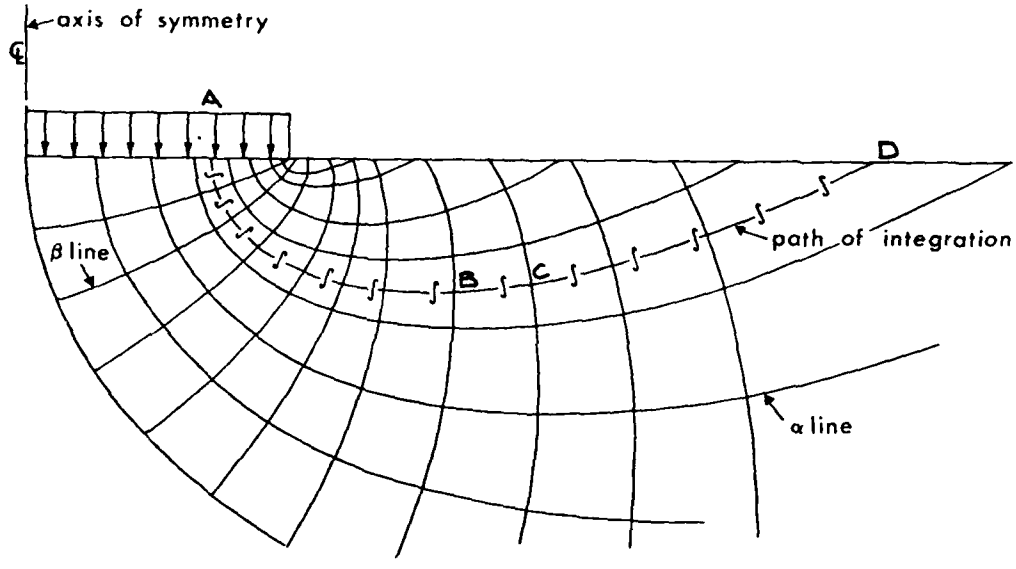

FIG. 2.4: *Axisymmetric Flow - an α,β net with Integration Path*

The numerical value of G for the flow tube ABCD is the path integral along Γ(ABCD), viz.

$$G\{\sigma'_\beta(\alpha)\} = \int_{\Pi} \frac{\delta\sigma_\beta}{\delta\alpha}\, e^{-\frac{\alpha-\alpha_o}{\alpha_t-\alpha}}\, d\alpha \qquad 2.7$$

$$\alpha_o \leq \alpha \leq \alpha_t$$

where α is the distance along the flow path measured from the source at α_o and α_t is the terminal point on path Π.

The flow tube cannot be taken in isolation because it is bounded by contiguous zones of the α,β net which are also in a state of compatible flow i.e. there are no discontinuities in the velocity across α - lines.

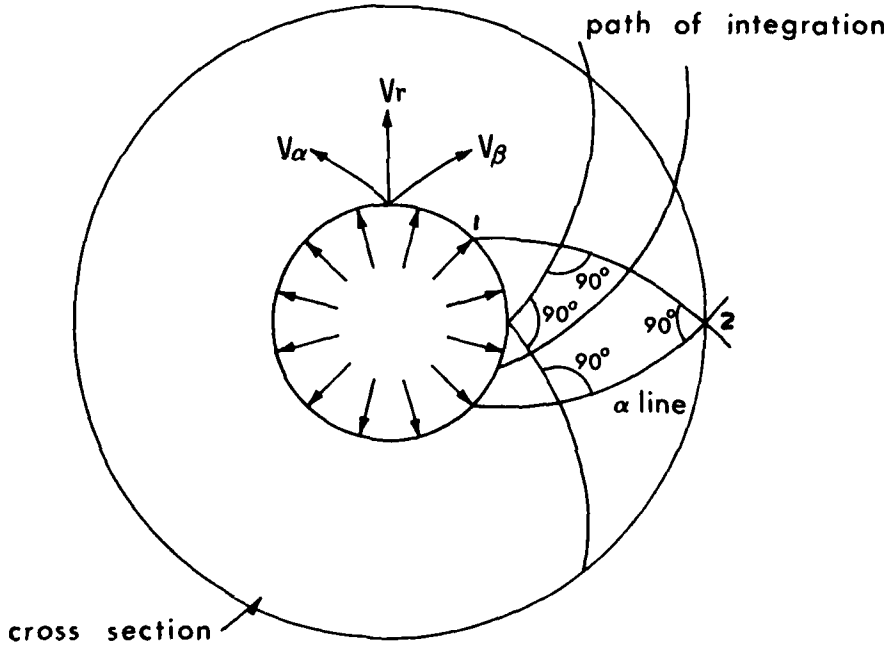

FIG. 2.5: *Radial Flow in Hollow Cylinder Test*

2.4 *Determination of the Displacement Field*

If a material is uncompressible the volume occupied is constant; the quantity of material which enters a sub-region is equal to that which leaves it according to the continuity equation of fluid mechanics

$$\frac{\delta v_x}{\delta x} + \frac{\delta v_y}{\delta y} + \frac{\delta v_z}{\delta z} = o \qquad 2.9$$

The movement of the material can be described in either Eularian or Lagrangian coordinates; in any case the relationship between the two systems is well established, Hodge pp. 143-144.

Due to the comparatively small scale of movements in a highly viscous medium the Lagrangian approach is deemed adequate for tracking the progress of flow from one zone to another; the change in stress gradiant is sufficiently small to warrant the adoption of a fixed reference frame. Thus we wlll focus on the relationship that expresses the displacements caused by flow of material into and out of a cell of a fixed α,β net. The displacements are to be determined along the median path which is midway between adjacent α - lines, i.e. the path ρ shown Fig. 2.6.

The method proposed is to use the properties of the Jacobian functional derivative for comparison of areas in the two-dimensional net and the relationship between curvilinear and rectangular coordinates for the third dimension of the flow tube. The constant volume

condition can be expressed in terms of the distribution of the Jacobiam along the flow path and the variation in area of the flow tube *normal* to direction of flow. With reference to Fig. 2.6 the relationship in terms of displacements is derived as follows:

Let J denote the Jacobian defined by*

$$J = Det \begin{vmatrix} \frac{\delta\alpha}{\delta x} & \frac{\delta\alpha}{\delta y} \\ \frac{\delta\beta}{\delta x} & \frac{\delta\beta}{\delta y} \end{vmatrix} \equiv \left| \frac{\delta(\alpha,\beta)}{\delta(x,y)} \right|$$

The numerical value of the Jacobian varies along the median and it is a regular function (non vanishing) as demonstrated in the next Chapter. Thus the displacement δ_β normal to the β - lines is given by the

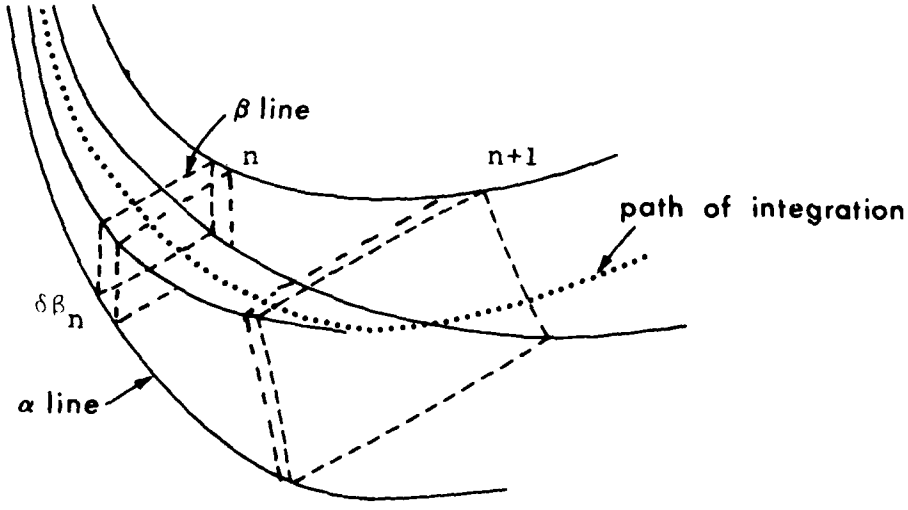

FIG: 2.6 *Sketch of Flow Tube*

* The topic of image mapping via the Jacobian transformation is discussed in Chapter 3 of this report. The family of curves $f(x,y) = \alpha$ and $g(x,y) = \beta$ are considered determinable entities at this stage.

expression

$$J_n \cdot A_n \cdot \delta\beta_n = J_{n+1} \cdot A_{n+1} \cdot \delta\beta_{n+1}$$

whence

$$\delta\beta_{n+1} = \frac{J_n \cdot A_n}{J_{n+1} \cdot A_{n+1}} \delta\beta_n. \qquad 2.10$$

The displacement of the centroid of a cell δs is given by the linear approximation:

$$\delta s_n = \frac{1}{2}(\delta\beta_n + \delta\beta_{n+1}) \qquad 2.11$$

where the notation is that shown in Fig. 2.6. On the boundary the displacement in a given interval of time due to surface traction reduces δ_{s_1} to δ_{β_1} if we take the first cell as a line element

i.e. $n = 1 \quad \delta\beta_1 = \delta s_1$

where δs_1 is deduced from the velocity as given by Equation 2.6. The Equations 2.10 and 2.11 enable tracking the values of displacements from the source of boundary perturbation to a terminal point on the boundary i.e. the exit of the material from the net.

To calculate the displacement it is necessary to have an expression for the cross sectional area of the flow tube at stations along the flow path. The relationships of the theory of curvilinear coordinates provide a general expression for the area, Marsden and Tromba (1975). pp 314.

viz. $$A(z) = \int_D \sqrt{\left|\frac{\delta(\alpha,\beta)}{\delta(x,y)}\right|^2 + \left|\frac{\delta(\alpha,\beta)}{\delta(y,z)}\right|^2 + \left|\frac{\delta(\alpha,\beta)}{\delta(x,z)}\right|^2}\, dx\, dy \qquad 2.12$$

where $A(z)$ denotes the area at any section

2.5 *Synthesis of Theoretical Formulations*

The foregoing analysis involved the hypothesis that the rate of flow can be related to the gradient of mean normal stress *a priori*. The mean normal stresses are considered spatially invariant with time and those values determined by linear elastic theory for constant boundary conditions. The notions of similitude and cross-correlation were applied to yield a dimensionally consistant relationship, i.e. equation 2.6. *In order* to establish a connection between the author's approach and orthodox analysis of flow problems, the governing differential equations for viscous flow is invoked. These classical equations collectively known as the Navier-Stokes equations are basic to analysis to both Newtonian and non-ideal fluids.

The Navier-Stokes equation for two-dimensional steady flow of an incompressible fluid with constant coefficient of viscosity η and density ρ reads:

$$\rho\left(\frac{\delta u}{\delta t} + u\frac{\delta u}{\delta x} + v\frac{\delta u}{\delta y}\right) + \frac{\delta p}{\delta x} - \eta\left(\frac{\delta^2 u}{\delta x^2} + \frac{\delta^2 u}{\delta y^2}\right) = 0$$

$$\rho\left(\frac{\delta v}{\delta t} + u\frac{\delta v}{\delta x} + v\frac{\delta u}{\delta y}\right) + \frac{\delta p}{\delta y} - \eta\left(\frac{\sigma^2 v}{\delta x^2} + \frac{\delta^2 v}{\delta y^2}\right) = 0 \qquad 2.13(a)$$

Where u and v are the velocity components in the x, y coordinate directions and p is the mean fluid pressure at a point (not a hydrostatic pressure) Chang Lu (1973). Equation 2.13(a) together with the continuity equation completes the classical formulation.

In the two-dimensional region the continuity equation is given by the expression:

$$\frac{\delta u}{\delta x} + \frac{\delta v}{\delta y} = 0$$

Neglicting acceleration but including inertial terms we have the expressions

$$\rho\left(u\frac{\delta u}{\delta x} + v\frac{\delta u}{\delta y}\right) - \eta\left(\frac{\delta^2 u}{\delta x^2} + \frac{\delta^2 u}{\delta y^2}\right) = -\frac{\delta p}{\delta x}$$

$$\rho\left(u\frac{\delta v}{\delta x} + v\frac{\delta v}{\delta y}\right) - \eta\left(\frac{\delta^2 v}{\delta x^2} + \frac{\delta^2 v}{\delta y^2}\right) = -\frac{\delta p}{\delta y} \qquad 2.13(b)$$

Under a coordinate transformation to another orthogonal frame of reference the property of invariance enables writing the equation 2.13(b) for the α,β coordinates in the form:

$$\rho\left(u\frac{\delta u}{\delta \alpha} + v\frac{\delta u}{\delta \beta}\right) - \eta\left(\frac{\delta^2 u}{\delta \alpha^2} + \frac{\delta^2 u}{\delta \beta^2}\right) = -\frac{\delta p}{\delta \alpha}$$

$$\rho\left(u\frac{\delta v}{\delta \alpha} + v\frac{\delta v}{\delta \beta}\right) - \eta\left(\frac{\delta^2 v}{\delta \alpha^2} + \frac{\delta^2 v}{\delta \beta^2}\right) = -\frac{\delta p}{\delta \beta} \qquad 2.13(c)$$

where now u and v are referred to the orthogonal spatial coordinates of the α,β net, and the term $\frac{\delta p}{\delta \alpha}$ is known from a separate analysis of the stress field.

The first equation of the set 2.13(c) only need be considered because the mean pressure gradient is zero everywhere within the solution domain for the right hand side of the second equation, i.e.

$$\frac{\delta p}{\delta \beta} \equiv 0$$

Furthermore $\frac{\delta u}{\delta \beta} \equiv 0$ therefore $\frac{\delta^2 u}{\delta \beta^2} = 0 \quad v = 0$

Thus the equation 2.13(c) reduces to an ordinary differential equation with respect to the α - lines, viz.

$$\eta \frac{d^2 u}{d\alpha^2} - \rho u \frac{du}{d\alpha} = \frac{dp}{d\alpha} \qquad 2.13(d)$$

writing the equation in the form

$$\eta \frac{d^2 u}{d\alpha^2} - \frac{1}{2} \rho \frac{d}{d\alpha} u^2 = \frac{dp}{d\alpha}$$

and integrating we obtain the Riccati differential equation

$$\eta \frac{du}{d\alpha} - \frac{1}{2} \rho u^2 - p(\alpha) = C_1 \qquad 2.13(e)$$

This nonlinear and non-homogeneous ordinary differential equation can be solved for u if a particular solution can be deduced, Courant and John (1974) Hidlebrand (1957). The general solution is formed from the known function by exponentiation and the ordinary process of integration with one arbitrary constant as given in Courant 1974. It appears that such solutions are mainly relevant in fluid mechanics or gravitational flow problems i.e. problems where the driving forces are derived from the gravitational influence on the mass density. However, it is significant to note that the displacements will have similar distributions whether equations 2.11 or 2.13(e)

are used. Finally the equation 2.13(e) has as its domain of independent variable α the path of integration inscribed on the physical flow line which is the same median path as that proposed for evaluating the correlation function $G\{\sigma_{\beta}^{1}\}$ of equation 2.7.

CHAPTER 3

Mapping Functions for Orthogonal Nets

3.1 *Flow nets: Approximation by Polynomials*

In this chapter a method for the functional representation of the geometry of orthogonal trajectories is presented. Families of orthogonal trajectories are encountered in hydraulic flow nets, electrostatics and stress fields, or indeed any physical problem described by Laplace's Equation. Flow nets are conventionally derived from the theory of complex variables in an exact formulation, approximated by the finite difference and finite elements techniques, or simply sketched freehand to match a particular set of boundary conditions. The generating functions deduced from complex variable theory can be quite complicated, while no functional representation emerges from the alternative methods. The problem as posed herein is to fit simple expressions which adequately describe the geometry in functional relationships.

The method proposed is that of trial fitting of polynomials where the selected polynomials consist of a set of harmonic mapping functions. These functions are generated from the definition of a complex function viz.

$$f(x,y) = (x + iy)^n : n = 1,2,3 \ldots; \; i = \sqrt{-1}$$

Thus by taking values of n to order 4 we obtain harmonic functions which are deemed to approximate the geometry of an orthogonal net. Letting ϕ and ψ represent the coordinates of a mapping function in a Cartesian frame of reference then the geometry is described by the relations:

$$\phi = A(2x+y) + B(x^2-y^2) + C(x^3-3xy^2) + D(x^4+y^4-6x^2y^2) + \phi_o$$

$$\psi = A(2y-x) + B(2xy) + C(3x^2y-y^3) + D(4x^3y-4y^3x) + \psi_o \qquad (3.1)$$

where A, B, C, D are scaling factors (real numbers).

The functions $\phi(x,y)$, $\psi(x,y)$ map a rectangular mesh into a distorted shape where the lines $x = c_1$, $y = c_2$ in the (x,y) plane appear as orthogonal trajectories in the (ϕ,ψ) space irrespective of the values of the sealing factors or the constants c_1, c_2. Now suppose that a plot of ϕ versus ψ in Cartesian coordinates is available from some source problem in electrostatics or ground water seepage. The task is to firstly find the origin of the generating functions $\phi(x,y)$, $\psi(x,y)$ if in fact the plot stems from a single origin, and second to extract the expressions that express the geometrical pattern in algebraic form. Assuming then that the net can be traced to a single origin, i.e. not bipolar or multipolar coordinate systems, the proposed analysis proceeds as follows:

1. A cell in (ϕ,ψ) space bounded by four intersecting trajectories is selected (remote from the confluence of lines that indicate a possible location of this origin of the coordinate system).
2. Simultaneous equations are written for the selected order of the harmonic functions by taking the nodes in turn with one of the four corner nodes as a temporary origin.
3. The set of simultaneous equations is solved for the

unknown values of the constants as given in Eqn. (3.1).

4. A search for those values of the constants which are consistent with the constraint that the coordinate intervals of (x,y) are restricted to integers is implemented.

5. The global origin with respect to the temporary origin is located by referring back to the results of the search of step 4 above.

Even in the case of a bipolar net the method can yield the functional relationships (at least locally) and it also may be applied to freehand plots in a piecewise scan of the net cells. Even freehand plots lead to well conditioned equations i.e. small changes in ϕ, ψ values are not grossly reflected in the values of the scaling factors.

The algebra can be considerably reduced by eliminating biquadratic terms, i.e. letting D = 0; this is a simplification that is well justified because of the ability of cubics to produce the optimum fit to an arbitrary continuous function (c.f. the theory of splines in succeeding chapter). Consider the plot of two functions ϕ and ψ in Cartesian coordinates as shown in Fig. 3.1. If we isolate any cell and select a temporary origin e.g. cell and the node marked 1 of inset in Fig. 3.1 we can write the coordinates of the nodes as

Node		
	1	(x_o, y_o)
	2	$(x_o, y_o + 1)$
	3	$(x_o + 1, y_o + 1)$
	4	$(x_o + 1, y_o)$

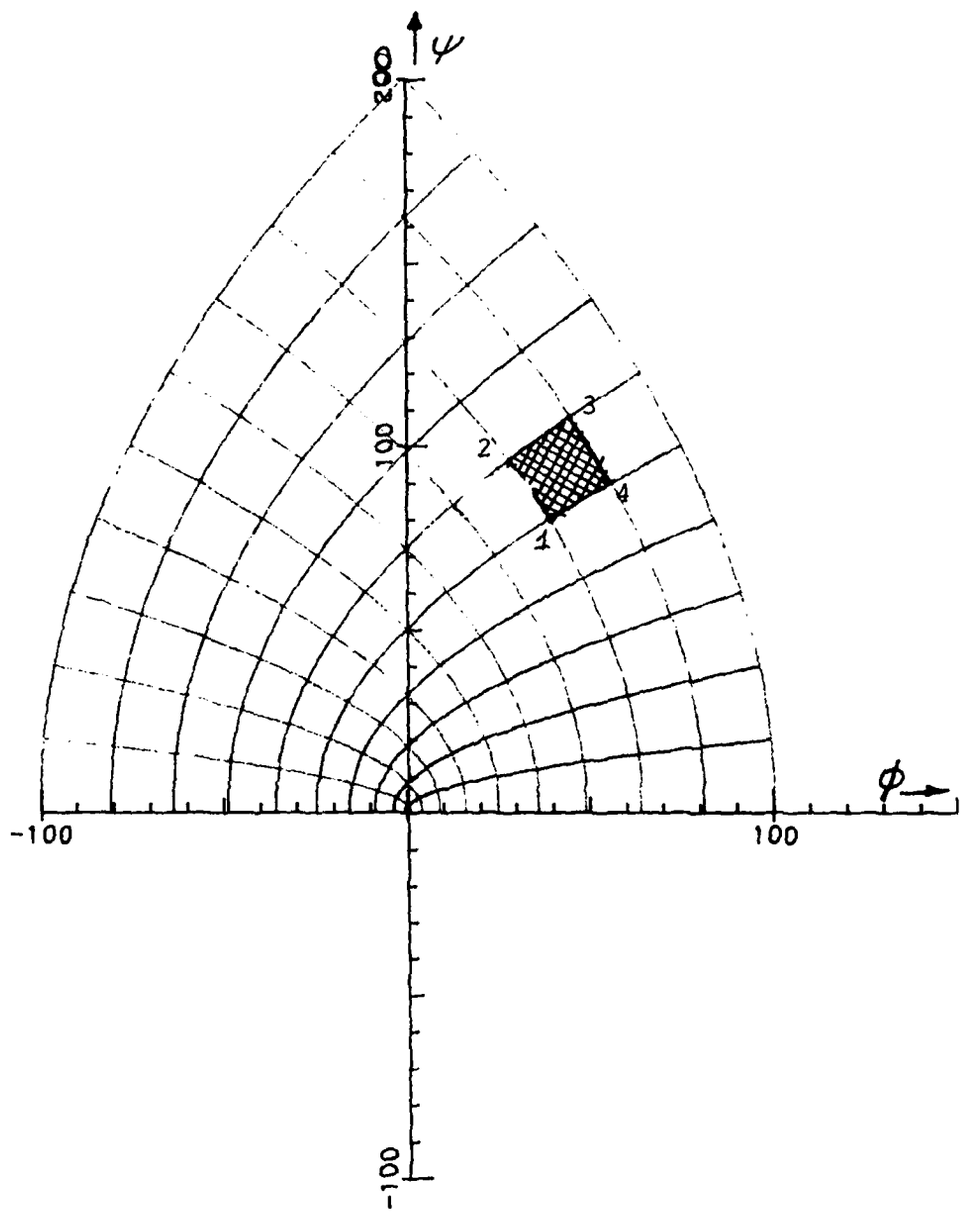

Fig. 3.1: *Orthogonal NET - No. 1*

where (x_o,y_o) are the specific Cartesian coordinates of the lower left hand node of the cell.
Substituting these ordered pairs in Equation (3.1) for the abbreviated cubic version we obtain the following:

Node 1

$$\phi_1 = A(2x_o+y_o) + B(x^2_o-y^2_o) + C(x^3_o-3x_oy^2_o) + \phi_o$$

$$\psi_1 = A(2y_o-x_o) + B(2x_oy_o) + C(3x^2_oy_o-y^3_o) + \psi_o$$

Node 2

$$\phi_2 = A(2x_o+y_o+1)+B(x^2_o-y^2_o-2y_o-1)+C(x^3_o-3x_oy^2-6x_oy_o-3x_o) + \phi_o$$

$$\psi_2 = A(2y_o-x_o+2)+B(2x_o+2x_oy_o)+C(x^2_o+3x^2_oy_o-y^2_o-3y^2_o-3y_o-1) + \psi_o \qquad (3.2)$$

and similarly for nodes 3 and 4. Knowing the values of ϕ and ψ at the nodes we can take any three of the above equations and solve for the constants A, B, C over a range of integer values of x_o,y_o. It transpires that if there is a unique set of values of the constants that satisfy all combinations of the equations for the nodal ϕ,ψ values throughout the net then a global origin exists for the particular net. The temporary origin at the unique values of x_o,y_o gives the clue to the location of global origin. The offsets are then ϕ_o and ψ_o in Equation 3.2.

Before a numerical example is presented it is worthwhile to take a look at closed mathematical solutions of the problem of inverting images. With the assistance of a mathematician, the author arrived at a specimen solution

of a comparatively simple mapping problem. The exercise was motivated by remarks in a textbook to the effect that it should always be possible to invert a mapping of continuous functions (according to Riemann's Theorem) given the image[1], Courant and John (1974).

The mapping selected is given by the harmonic functions

$$\phi = x^2 + 4x - y^2 + 2y$$
$$\psi = 2xy + 4y - 2x$$

To find the inverse we must be able to find

$$x = f_1(\phi,\psi), \quad y = f_2(\phi,\psi)$$

Now $\phi = (x+2)^2 - (y-1)^2 - 3$

or $\phi+3 = X^2 - Y^2$ where $X = (x+2)$, $Y = (y-1)$

and $\psi = 2y(x+2) - 2(x+2) + 4$

or $\frac{\psi-4}{2} = XY.$ whence $Y = \frac{\psi-4}{2} \Big/ X$

$$\therefore \quad X^2(\phi+3) = X^4 - \left(\frac{\psi-4}{2}\right)^2$$

or $$X^4 - (\phi+3)X^2 - \left(\frac{\psi-4}{2}\right)^2 = 0$$

---

(1) It should be noted that while Riemann's mapping theorem demonstrates the existance of a mapping function, it does not actually produce the function.

$$X^2 = \frac{\phi+3 \pm \sqrt{(\phi+3)^2 + (\psi-4)^2}}{2} = (x+2)^2$$

$$x = \left\{\frac{\phi+3 \pm \sqrt{(\phi+3)^2 + (\psi-4)^2}}{2}\right\}^{1/2} - 2 = f_1(\phi,\psi)$$

$$y = \frac{\psi-4}{2X(\phi,\psi)} + 1 = f_2(\phi,\psi) \qquad 3.3(b) \qquad \text{Q.E.D.}$$

It is instructive to refer to Courant and John's text (or similar treatise) to see just how difficult the problem can become for the general case of image mapping, and indeed a numerical procedure is proposed as the most appropriate method.* Even in the case of the simple mapping investigated above the quadratic form of the inverse image precludes finding a unique mapping in the (x,y) plane. Indeed the effort required to extend the closed form approach to harmonic functions involving cubics is considerable as evidenced in attempts to apply Descartes method for solving cubic polynomial equations. Fortunately the reverse image is ameniable to numerical analysis. The numerical technique is easily programmed and although it would be impracticable to present the computer output in full abridged results serve the purpose of highlighting the main features of the numerical scheme. In what follows two typical cells are selected from a flow net, the net is shown in Fig. 3.2, and the values of ϕ and ψ are read from the geometry of the net referred to Cartesian coordinates.

---

* The numerical method merely enables mapping in the neighborhood of an isolated point and hence it is of limited usefulness.

3.2 *Example of Decoded Flow Net*

Suppose that part of a net which does not include an origin (source or sink) is given in rectangular co-ordinates (x,y). The problem posed is one of extracting the analytic function that represents the entire region of the net i.e. to find the function

$$\zeta = \phi(x,y) + i\psi(x,y)$$

where ϕ and ψ are assumed continuously differentiable functions (excepting the neighbourhood of the origin). A successful outcome of the exercise will enable plotting the net over any region of interest and it will also provide the Jacobian in algebraic form. A condition for computational success is that the mesh is uniformly divergent from its origin. The analysis of this problem by the method of polynomial harmonic functions is demonstrated with the aid of a computer generated mesh as shown in Fig. 3.2. This net was plotted by assigning values to the constants A,B,C in Equation 3.2. Although the answer is known beforehand the main features of the approach is illustrated by selecting a precisely drawn net.

The known values of ϕ and ψ provide eight algebraic equations per cell. These equations will in general be non-linear in terms of (x,y) coordinates. However as the (x,y) values can be treated as parameters, each taking on integer values only, the Equations 3.2 can be programmed within a loop over a range of the integers. Such a search will yield the values of (x,y) relative th a common origin for which the constants A, B, C and D are invariant with respect to the position of the cell.

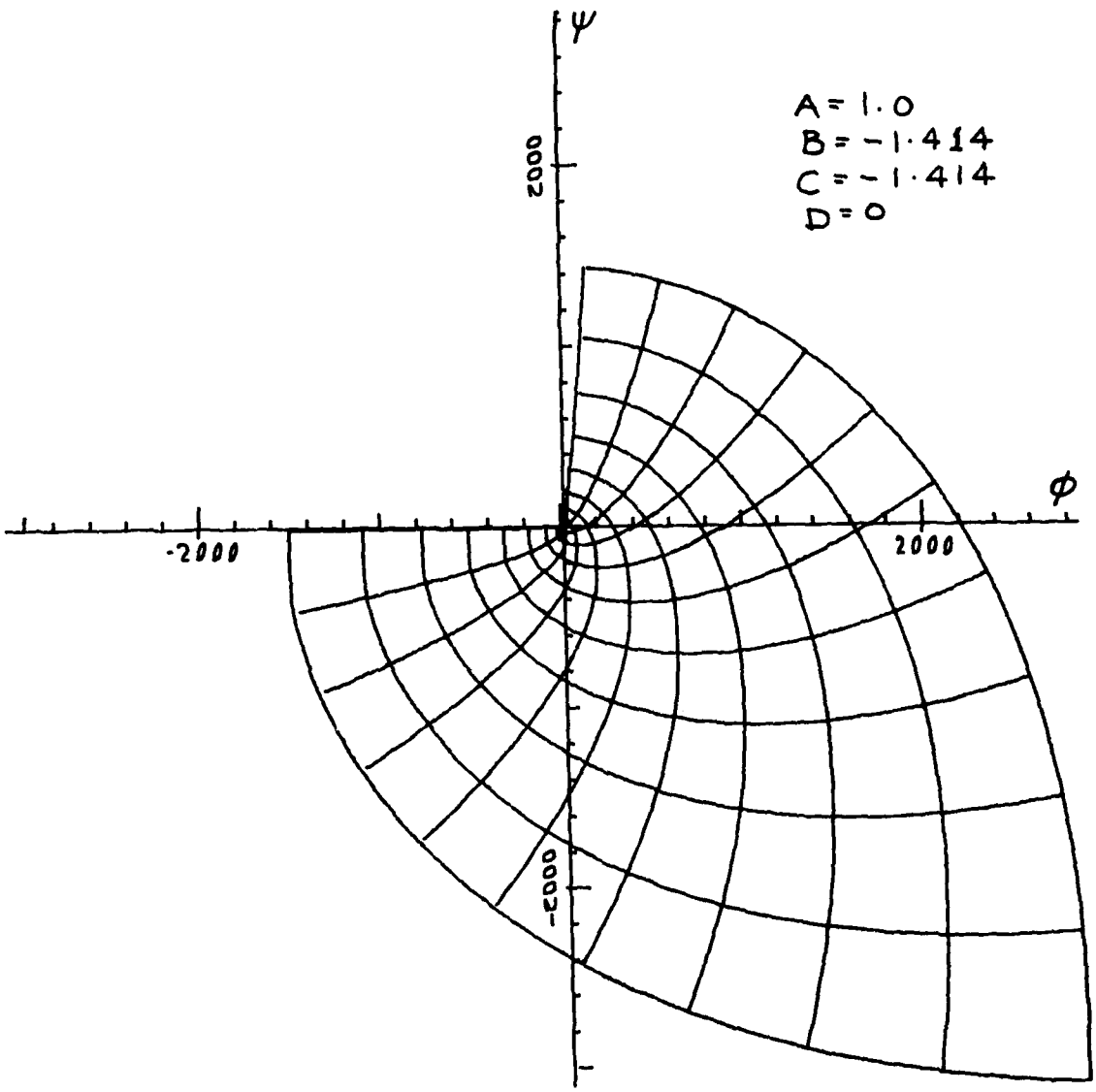

Fig. 3.2: *Orthogonal Net - No. 2.*

Cubic and quartic interpolation schemes are handled with equal ease, so the search for a unique set of constants applicable to each of the cells can commence with a cubic polynomial approximation. The mapping is illustrated in Fig. 3.3.

Thus we can write sets of simultaneous equations for the nodes 1 to 4 as follows:

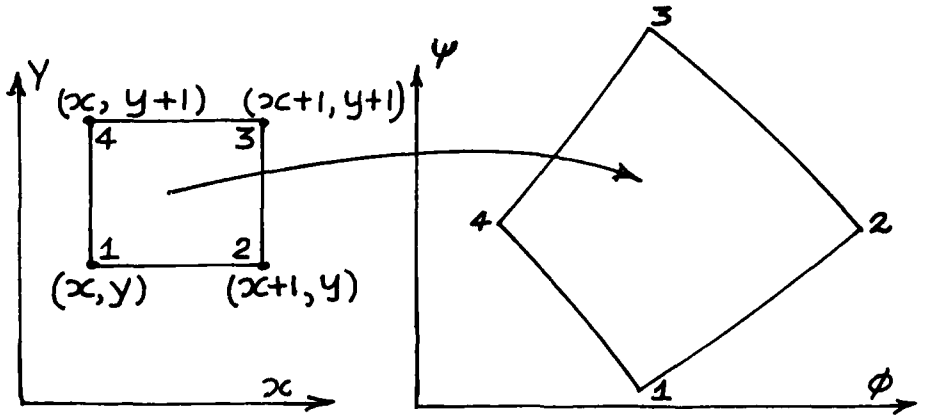

FIG. 3.3 *Typical cell of Orthogonal net*

SET I

$\Phi_1 = A(2x+y) + B(x^2-y^2) + C(x^3-3xy^2)$

$\psi_1 = A(2y-x) + B(2xy) + C(3x^2y-y^3)$

$\phi_4 = A(2x+y+1) + B(x^2-y^2-2y-1) + C(3x^2y+3x^2-y^3-3y-1)$

SET II

$\phi_2 = A(2x+y+2) + B(x^2+2x+1-y^2) + C(x^3+3x^2+3x+1-3xy^2-3y^2)$

$\psi_2 = A(2y-x-1) + B(2xy+2y) + C(3x^2y+6xy+3y-y^3)$

$\psi_4 = A(2y+2-x) + B(2xy+2x) + C(3x^2y+3x^2-y^3-3y^2-3y-1)$

SET III

$\phi_4 = A(2x+y+1) + B(x^2-y^2-2y-1) + C(x^3-3xy^2-6xy-3x)$

$\psi_4 = A(2y+2-x) + B(2xy+2x) + C(3x^2+3x^2-y^3-3y^2-3y-1)$

$\phi_2 = A(2x+y+2) + B(x^2+2x+1-y^2) + C(x^3+3x^2+3x+1-3xy^2-3y^2)$

SET IV

$\phi_2 = A(2x+y+2) + B(x^2+2x+1-y^2) + C(x^3+3x^2+3x+1-3x+1-3xy^2-3y^2)$

$\phi_1 = A(2x+y) + B(x^2-y^2) + C(x^3-3xy^2)$

$\phi_4 = A(2x+y+1) + B(x^2-y^2-2y-1) + C(x^3-3xy^2-6xy-3x)$

SET V

$\psi_2 = A(2y-x-1) + B(2xy+2y) + C(3x^2y+6xy+3y-y^3)$

$\psi_1 = A(2y-x) + B(2xy) + C(3x^2y-y^3)$

$\psi_4 = A(2y+2-x) + B(2xy+2x) + C(3x^2y+3x^2-y^3-3y^2-3y-1)$

The equations above are solved for the constants A, B and C by inserting values of ϕ and ψ at the nodes and a range of integer values for x and y; the process is continued until a particular pair of x,y values yield the same values for the constants irrespective of the ordering of the set of equations. The consistent values are identified in Table III-1 by arrows in right hand margin. Because of re-ordering of node numbers in programs run on the Hewlett Packard and Digital computers the diagrams are at some variance with the tabulated results. Nevertheless, the results as listed, the program in BASIC, demonstrates the key features of the analysis.

Cell i Nodal values	SET I			SET II			SET III			x_o, y_o	
	A	B	C	A	B	C	A	B	C		
ϕ_1 = 368	-15.14	-4.18	-1.35	-12.46	-5.22	-1.41				4,6	
ψ_1 = -419	14.52	-2.12	-1.60	12.30	0.0	-1.88				5,4	
ϕ_2 = 618	1.00	-1.41	-1.41	1.00	-1.41	-1.41	1.00	-1.41	-1.41	5,5	◁
ψ_2 = -409	-10.97	-0.66	-1.29	-8.49	-1.83	-1.12	-20.92	1.12	-1.64	5,6	
ϕ_4 = 330	10.83	3.71	-1.68	8.25	5.98	-1.93				6,4	
ψ_4 = -668											

Cell j	SET III			SET IV			SET V				
	A	B	C	A	B	C	A	B	C		
ϕ_1 = 229	-33.40	-1.67	-1.72	-16.08	-7.03	-1.19	+59.93	-15.64	-0.46	6.7	
ψ_1 = -1056	+25.17	-4.20	-1.31	+4.68	+5.26	-2.01	+63.27	-7.77	-1.15	7,5	
ϕ_2 = 480	1.00	-1.41	-1.41	1.00	-1.41	-1.41	1.00	-1.41	-1.41	7,6	◁
ψ_2 = -1455	-26.06	+1.67	-1.59	-6.29	-4.98	-1.05				7,7	
ϕ_4 = 991	+21.02	+1.29	-1.40	+6.00	+7.86	-1.82					

TABLE III-I *Abridged Results of Computer Output*

The results, determined for cells i and j, are given in Table III-I where the constants for a partial list of the independent parameters are tabulated.

The position of the global origin is at the same location for the two cells chosen here:

Cell $\underline{i}$: origin : x = 5 and y = 5
Cell $\underline{j}$: origin : x = 7 and y = 6
Constants A = 1.00, B = -1.41, and C = -1.41, D = 0.

The results can be verified for all cells outside the immediate vicinity of the origin i.e. where the change is curvature is moderate. The equation of the entire net are now established in the relationships

$$\phi = =2x+y-1.41(x^2-y^2)-1.41(x^3-3xy^2)$$
$$\psi = 2y-x-2.82(xy)-1.41(3x^2y-y^3)$$

and the analytical function ζ is completely defined. The flow net can be extended indefinitely by using these functions.

However in stress analysis the relationship is normally encountered with form $\psi = f(\phi)$. Thus equation 3.3 would be reduced to:

$$\psi = 2X(X^2-\phi-3)^{\frac{1}{2}} + 4 \qquad (X = x+2) \qquad 3.3.c$$

On a Cartesian plot the expression $\psi = f(\phi)$, for a specific domain of $\phi(x,y)$, is a family of curves because ψ is a multivalued function if we vary x or y. The curvilinear plot is more readily described in curvilinear coordinates wherein the points set (x,y) are regarded as curvilinear coordinates. From this viewpoint the differential relationship for areas of cells is given by the expression

$$d\phi d\psi = |J| dx\ dy$$

where $|J|$ is the determinant of the Jacobian matrix.

The value of the Jacobian is given by the expression

$$|J| = \frac{\delta\phi}{\phi x} \cdot \frac{\delta\psi}{\delta y} - \frac{\delta\phi}{\delta y} \cdot \frac{\delta\psi}{\delta x} \qquad 3.4$$

Hence for cubic interpolation

$$|J| = 5A^2+8ABx+12ACx^2-12ACy^2+4B^2x^2+4B^2y^2-4ABy+$$
$$12BCx^3+12BCxy^2+9C^2x^4+18C^2x^2y^2+9C^2y^4-12ACxy \qquad 3.5$$

For interpolation up to and including quartic terms (n=4) the Jacobean is given by the following terms inserted in Equation 3.4 :-

$$\frac{\delta\phi}{\delta x} = 2A + 2Bx + 3C(x^2 - y^2) + 4D(x^3 - 3xy^2)$$

$$\frac{\delta\phi}{\delta y} = A - 2By - 6Cx + 4D(y^3 - 3x^2y) \qquad 3.6$$

By Cauchy-Riemann relationships

$$\frac{\delta\psi}{\delta y} = \frac{\delta\phi}{\delta x}$$

$$\frac{\delta\psi}{\delta x} = -\frac{\delta\phi}{\delta y}$$

Equation 3.4 is easily evaluated.

3.3 *Areas of Cells*

The Jacobian transformation provides a convenient method for finding the areas of individual cells of a flow net. Alternative methods are based on co-ordinate geometry via subdivision and Gaussian quadrature. Because we require an accurate assessment of the area to calculate the quantities appearing in Equations 2.10 and 2.11 an investigation of the accuracy of the various methods for finding area was undertaken. The flow net shown in Fig. 3.4 was adopted for this exercise.

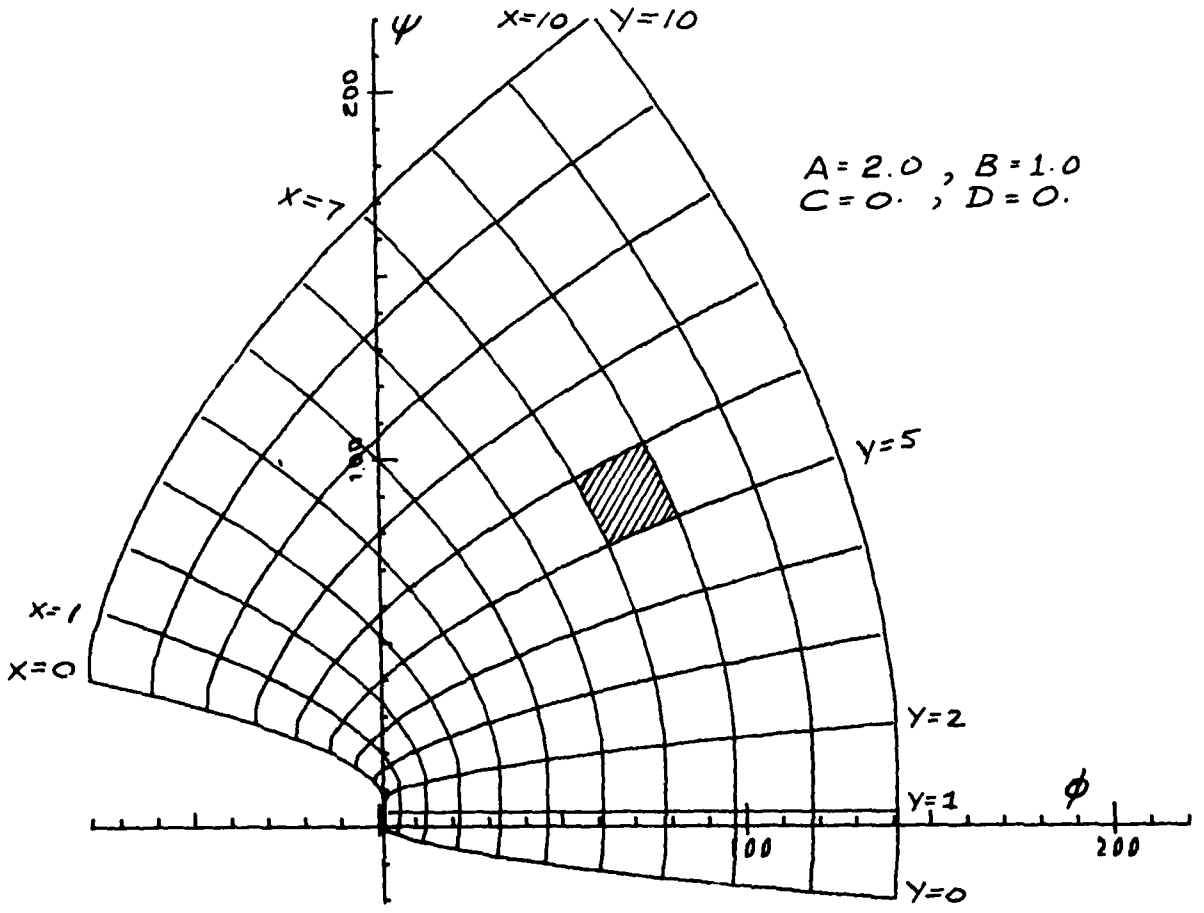

Fig. 3.4 *Orthogonal Net for Cell Area*

The Jacobian method follows from the expression for the the area:

$$A = |J| * \Delta x * \Delta y$$

where J is the Jacobian taking on the lowest values of the (x,y) co-ordinates of the given cell. The maximum values of Δx (and Δy) equals unity so convergence can be tested by subdividing the cell into smaller areas, say $\Delta x = 0.1$, $\Delta y = 0.1$, and summing the subareas.

Gaussian quadrature using two and three point interpolation is the most commonly used numerical scheme. The weighting factors are given in Table III-2 and the area is obtained from the expression

$$A = \sum_{j=1}^{m} \sum_{i=1}^{m} w_i * w_j * F(a_i, b_j) + E \qquad 3.6$$

where m = order of the integration rule

w_i = weights

a_i, b_i = abscissae of integration points

F = function values

E = error in approximation

TABLE III-2 *Abscissas and weights for Legendre-Gauss Quadrature (of order 4).*

Interval |-1,1|

m	Abscissae	Weight
2	±0.557350	1
3	0	8/9
	±0.7774597	5/9
4	±0.339981	0.652145
	±0.861136	0.347855

Interval |0,+1|*		
4	0.06943	0.34785
	0.33000	0.65214
	0.69999	0.65214
	0.93056	0.34785
5	0.04691	0.23692
	0.23076	0.47862
	0.5000	0.56888
	0.76933	0.47862
	0.95308	0.23692

For the curvilinear square shown in Fig. 3.4 with origin at $x = 7$, $y = 5$ the four point quadrature over the interval $|0, +1|$ gives an area of 442.60 units.

The results for cubic interpolation using Equation 3.5 are as follows

Number of Subdivisions	Area of Cell
Nil	388.00
2	415.00
4	428.75
5	431.52
10	437.08

By taking the Jacobian determinant at the point $x = 7.5$, $y = 5.5$ (and no subdivisions) the value obtained for the area is 442.00 units.

---

* The Legendre-Gauss coefficients for the interval $|0,+1|$ were calculated by Al-Salihi (1978).

Hence it appears from the quantities underlined in above that the Jacobian determinant evaluated at the intersection of the medians to the sides gives a good estimate for the asymptotic value of the area projected by subdividing the cell. Where the Jacobian can be determined analytically it proves more expeditious than quadrature formulae which in itself is a motivation for trying to fit polynomials to flow nets.

3.4 *The Conjugate Function*

The foregoing theory pertains to conformal mapping from one plane to another. At this juncture it is relevant to compare the geometrical exercise with its physical counterparts, namely, the derivation of velocity potential and stream functions in fluid mechanics, or the plotting of equipotential and flow lines in electrostatics and soil mechanics. In these problems it often transpires that one of the functions is more readily plotted than the other on physical grounds. For instance as an example of a potential function let the distribution of the potential be denoted by ϕ (which is analogous to the previous interpretation of ϕ as a curve in the plane of Cartesian space) where ϕ is a known function of position in the solution domain in the x-y plane. In this instance ϕ represents the distribution of a potential such as pore pressure, voltage or magnetic flux. Take for example the real part of the harmonic function

$$\phi = x^2 + 4x - y^2 + 2y$$

where ϕ satisfied Laplace's equation,

$$\frac{\delta^2\phi}{\delta x^2} + \frac{\delta^2\phi}{\delta y^2} = 0$$

The conjugate function must satisfy

$$\frac{\delta^2\psi}{\delta x^2} + \frac{\delta^2\psi}{\delta y^2} = 0$$

The function ψ is deduced from the expression

$$\psi = \int_{y_o}^{y} \frac{\delta\phi}{\delta x}\, dy. - \int_{x_o}^{x} \left(\frac{\delta\phi}{\delta y}\right)_{y=y_o} dx \qquad 3.6$$

In this example

$$\psi = 2\int_{y_o}^{y} (x+2)\,dy + 2\int_{x_o}^{x} |(y-1)|_{y=y_o}\, dx$$

$$= 4y - 2x + 2xy + c$$

where $c = 2(x_o - x_o y_o - 2y_o)$

Thusly the real and imaginary parts of an analytic function are evaluated. However, this simple example merely serves to demonstrate the method of conjugate functions; in practical examples the process can become very difficult. A general method using finite difference approximations on a curvilinear orthogonal grid combined with an analytic solution has been reported by Centurioni and Viviani (1975).

The discource in this Chapter leads to the conclusion that mapping functions can be deduced by inspection of the constraints in a problem. The initial trials can be adjusted to approximate flow paths in the

areas of fluid and soil mechanics, diffusion process and electrostatics. Experience of generating orthogonal nets by simply varying the parameters in a cubic polynomial representation suggests that a useful technique has been introduced. By using the computer generated plots to overlay a given potential field the functional relationships can be determined piecewise, or in favourable circumstances the mathematical description of the entire field.

We have performed these exercises on a variety of flow nets with the result that it has always been found possible to locate the origin if the net had been accurately drawn from a single origin. The values listed in Table III-I indicate that the sets are distinct, leading to well conditioned simultaneous equations. The main drawback to this approach is the stipulation of a unique origin of the net. It will be seen in the further development of our analysis that this requirement can be relaxed albeit at the expense of computational effort. A further drawback is due to the fact that the conjugate function Ψ is not an even function, as may be seen by inspection of Equation 3.1. Therefore it results in plots with skew symmetry which limits class of problems to which the nets may be applied. The only symmetric plot results from the quadratic terms of Equation 3.1.

Negative integers employed as the exponents in the analytic function lead to cumbersome algebra in the Jacobian determinant, and hence taking $n < 0$ confers no practical advantage.

CHAPTER 4

CUBIC INTERPOLATORY SPLINES

4.1 *Introduction*

The theory of splines is well documented so only a brief review is presented herein as a background to the development of a computer program for parametric cubic spline interpolation of material flow paths.

Splines are an important tool in modern numerical analysis for

1) Interpolation
2) Numerical integration and differentiation
3) Numerical solutions of ordinary differential equations
4) Numerical solutions of partial differential equations.

However the interpolatory property of the splines is only of interest here. The great advantage of splines in interpolation is that they do not have the oscillatory property of the interpolating polynomial. The most widely used splines are the cubic splines.

4.2 *Definition of a Cubic Spline*

A cubic spline S(t) with modes t_i, t_2 ..... t_n ($t_i < t_2 < t_3 ..... < t_n$) is a function which in the interval $t_i \leq t \leq t_i + 1$ ($i = 1,2, ... n-1$) reduced to a cubic polynomial in t, and at each interior node t_i ($i = 2,2,...n-1$), S(t), S'(t) and S''(t) are continuous function and its derivatives.

Such a function may be represented in the interval $t_i \leq t \leq t_i + 1$ $(i = 1,2,...n-1)$ in the form

$$S_i = F(t) = a_i t^3 + b_i t^2 + c_i t + d_i$$

where, associated with each cubic arc S_i, there are four unknown coefficients a_i, b_i, c_i and d_i. It follows that there are 4 (n-1) conditions to be fulfilled, so that S(t) is fully defined mathematically

1) S(t) must match at the interval nodes
   $S(t_i) = T(t_i)$
   i.e. n equations
2) S(t) must be continuous over the boundaries
   $S(t_{i-}) = S(t_{i+})$ $i = 2(1)n-1$
   i.e. n-2 equations
3) S'(t) and S''(t) must be continuous over the boundaries
   $S'(t_{i-}) = S'(t_{i+})$
   $S''(t_{i-}) = S''(t_{i+})$ $i = 2(1)n-1$
   i.e. 2n-4 equations

Hence there are 4n-6 equations with 4n-4 unknowns. To overcome this problem the natural cubic spline can be employed which has the extra condition for the second derivatives

4) $S''(t_1) = 0$
   $S''(t_n) = 0$

This corresponds to letting the physical spline project past the end weights. Usually one is not interested in $t < t_i$ or $t > t_n$ but if they arise the natural spline is

extended by straight lines agreeing in value and slope at the ends t_i and t_n.

The second derivative is then also continuous at the ends. Hence there are two more equations to deduce 4n-4 equations to solve for 4n-4 unknowns. Thus the mathematical spline is explicitely defined.

Condition (1) implies that the curve goes through the knots, or nodes. Conditions (2) and (3) imply continuity of alignment, continuity of slope and continuity of curvature respectively.

In contrast to polynomial interpolation which increases the degree to interpolate more points, here the degree is fixed and one uses more polynomials instead - one for each interval. For each interval the natural cubic spline is unique and is the smoothest interpolating curve through these points.

4.3 *Derivation of the Natural Cubic Spline*

For notational convenience let

$$h_i = t_{i+1} - t_i$$

$$S_i(t) = S^{(t)},\ t\varepsilon\left|t_i, t_{i+1}\right|$$

$$M_i = S''(t_i)$$

Because $S_i(t)$ is a cubic polynomial the second derivative $S_i''(t)$ is a linear polynomial and can be expressed in the form

FIGURE 4.1

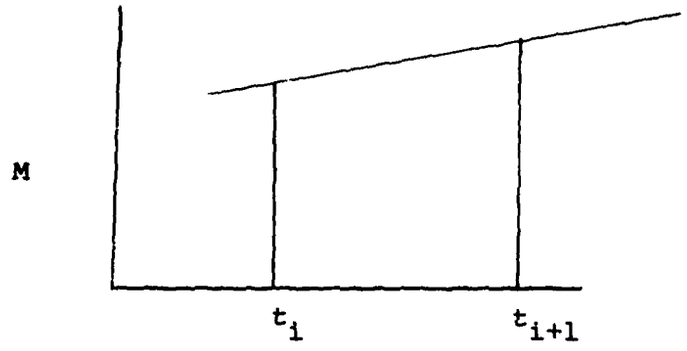

$$S_i''(t) = \frac{M_i}{h_i}(t_{i+1}-t) + \frac{M_{i+1}}{h_i}(t-t_i) \qquad (4.1)$$

$$i = 1(1)n-1$$

To obtain expressions for $S_i(t)$ equation (4.1) is integrated twice giving

$$S_i(t) = \frac{M_i}{6h_i}(t_{i+1}-t)^3 + \frac{M_{i+1}}{6h_i}(t-t_i)^3 + At + B$$

where A and B are constants

To determine A and B conditions (1) states that

$$S_i(t_i) = F(t_i)$$

$$S_i(t_{i+1}) = F(t_{i+1})$$

$$S_i(t_i) = F(t_i) = \frac{M_i}{6h_i}(t_{i+1}-t_i)^3 + \frac{M_{i+1}(t_i-t_i)^3}{6h_i} + At_i + B$$

$$S_i(t_i) = F(t_i) = \frac{M_i h_i^2}{6} + At_i + B$$

$$S_i(t_{i+1}) = F(t_{i+1}) = \frac{M_i}{6h_i}(t_{i+1}-t_{i+1})^3 + \frac{M_{i+1}}{6h_i}(t_{i+1}-t_i)^3 + At_{i+1} + B$$

or

$$S_i(t_{i+1}) = F(t_{i+1}) = \frac{M_{i+1}h_i^2}{6} + At_{i+1} + B$$

FIGURE 4.2

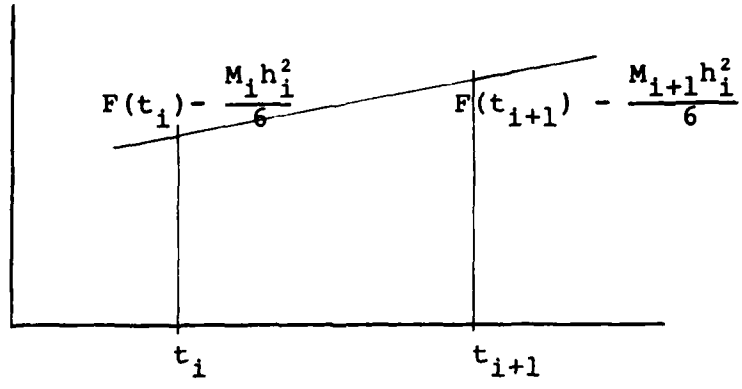

By linear interpolation (Fig. 4.2)

$$At + B = \{F(t_i) - \frac{M_i h_i^2}{6}\} \frac{(t_{i+1}-t)}{h_i} + \{F(t_{i+1}) - \frac{M_{i+1}h_i^2}{6}\} \frac{(t-t_i)}{h_i}$$

This leads to the following expression for $S_i(t)$

$$S_i(t) = \frac{M_i}{6h_i}(t_{i+1}-t)^3 + \frac{M_{i+1}}{6h_i}(t-t_i)^3 + \{F(t_i) - \frac{M_i h_i^2}{6}\}\frac{(t_{i+1}-t)}{h_i} + \{F(t_{i+1}) - \frac{M_{i+1}h_i^2}{6}\}\frac{(t-t_i)}{h_i} \qquad (4.2)$$

$$i = 1,2, \ldots (n-1)$$

The condition of slope continuity leads to a recursive equation for the unknowns i.e. the second derivatives.

To find $M_{(s)}$ the condition that the first derivative of $S_i(t)$ is continuous throughout is used

$$\text{i.e. } S'_{i-1}(t_i) = S'_i(t_i) \qquad i = 2,3..n$$

Differentiating equation (4.2) yields

$$S'_i(t) = \frac{M_i}{2h_i}(t_{i+1}-t)^2 + \frac{M_{i+1}}{2h_i}(t-t_i)^2 + \frac{F(t_{i+1})-F(t_i)}{h_i} - \frac{h_i}{6}(M_{i+1}-M_i)$$

$$S'_{i-1}(t_i) = \frac{M_{i-1}}{2h_{i-1}}(t_i-t_i)^2 + \frac{M_i}{2h_{i-1}}(t_i-t_{i-1})^2 + \frac{F(t_i)-F(t_{i-1})}{h_{i-1}} - \frac{h_{i-1}}{6}(M_i-M_{i-1})$$

$$= \frac{M_i}{2h_{i-1}}h_{i-1}^2 + \frac{F(t_i)-F(t_{i-1})}{h_{i-1}} - \frac{h_{i-1}}{6}(M_i-M_{i-1}) \quad (4.3)$$

$$S'_i(t_i) = -\frac{M_i}{2h_i}(t_{i+1}-t_i)^2 + \frac{F(t_{i+1})-F(t_i)}{h_i} - \frac{h_i}{6}(M_{i+1}-M_i)$$

$$= -\frac{M_i}{2h_i}h_i^2 + \frac{F(t_{i+1})-F(t_i)}{h_i} - \frac{h_i}{6}(M_{i+1}-M_i) \quad (4.4)$$

Let $F(t_i) = F_i$

Equating (4.3) to (4.4) gives

$$\frac{M_i h_{i-1}^2}{2h_{i-1}} + \frac{F_i-F_{i-1}}{h_{i-1}} - \frac{h_{i-1}}{6}(M_i-M_{i-1})$$

$$= -\frac{M_i h_i^2}{2h_i} + \frac{F_{i+1}-F_i}{h_i} - \frac{h_i}{6}(M_{i+1}-M_i)$$

which gives

$$M_{i-1}\frac{(h_{i-1})}{h_i} + 2M_i\frac{(h_i+h_{i-1})}{h_i} + M_{i+1}$$

$$= \frac{6}{h_i}\left\{\frac{F_{i+1}-F_i}{h_i} - \frac{F_i-F_{i-1}}{h_{i-1}}\right\}$$

$$i = 2,3 \ldots (n-1)$$

By definition of the natural cubic spline M_i and M_n are zero. For the intervals (t_i,t_2) and (t_{n-1},t_n) the above equation reduces to

$$2M_2\frac{(h_2+h_1)}{h_i} + M_3 = \frac{6}{h_2}\left\{\frac{F_3-F_2}{h_2} - \frac{F_2-F_1}{h_i}\right\}$$

$$M_{n-2}\left\{\frac{h_{n-2}}{h_{n-1}}\right\} + 2M_{n-1}\left\{\frac{h_{n-1}-h_{n-2}}{h_{n-1}}\right\} = \frac{6}{h_{n-1}}\left\{\frac{F_n-F_{n-1}}{h_{n-1}}\right.$$

$$\left. - \frac{F_{n-1}-F_{n-2}}{h_{n-2}}\right\}$$

Writing the equation for all the intervals gives the Equations 4.5 as shown on the next page.

$$
\begin{bmatrix}
2\frac{(h_2+h_1)}{h_i} & 1 & 0 & \cdots & 0 \\
\frac{h_2}{h_3} & 2\frac{(h_3+h_2)}{h_3} & 1 & \cdots & 0 \\
0 & \frac{h_3}{h_4} & 2\frac{(h_4+h_3)}{h_4} & 1 & 0 \\
0 & \frac{h_{i-1}}{h_i} & 2\frac{(h_i+h_{i-1})}{h_i} & 1 & \\
 & & & 0 & \\
 & & & 1 & \\
0 & & \frac{h_{n-2}}{h_{n-1}} & 2\frac{(h_{n-1}-h_{n-2})}{h_{n-1}} &
\end{bmatrix}
\begin{bmatrix} M_2 \\ M_3 \\ M_4 \\ M_i \\ \\ \\ M_{n-1} \end{bmatrix}
=
$$

$$
\begin{bmatrix}
\frac{6}{h_2}\left\{\frac{F_3-F_2}{h_2} - \frac{F_2-F_1}{h_1}\right\} \\
\frac{6}{h_3}\left\{\frac{F_4-F_3}{h_3} - \frac{F_3-F_2}{h_2}\right\} \\
\frac{6}{h_i}\left\{\frac{F_{i+1}-F_i}{h_i} - \frac{F_i-F_{i-1}}{h_{i-1}}\right\} \\
\frac{6}{h_{n-1}}\left\{\frac{F_n-F_{n-1}}{h_{n-1}} - \frac{F_{n-1}-F_{n-2}}{h_{n-2}}\right\}
\end{bmatrix}
\qquad 4.5
$$

This gives a system of tri-diagonal linear equations which are diagonally dominent. This system of equations may be solved by using the Thomas alogrithm or by any method for solving linear equations. However one can generate a recursive algorithm to solve for the M_s, Sampine and Allen (1973).

Let $d_i = \frac{6}{h_i}\left(\frac{F_{i+1}-F_i}{h_i} - \frac{F_i-F_{i-1}}{h_{i-1}}\right)$

and let $M_{i-1} = \rho_i M_i + \tau_i \qquad i = 2,3,\ldots n \qquad (4.6)$

Where the values for ρ_i and τ_i must be found.

$M_1 = 0$ therefore one may assume that ρ_1 and $\tau_1 = 0$.

Substituting (4.6) into (4.5) gives

$$\frac{h_{i-1}}{h_i}(\rho M_i+\tau_i) + 2\left\{1+\frac{h_{i-1}}{h_i}\right\}M_i+M_{i+1} = d_i$$

$$\text{or } \left\{\frac{h_{i-1}}{h_i}\rho_i + 2\left\{1+\frac{h_{i-1}}{h_i}\right\}\right\} M_i+M_{i+1} = d_i - \frac{h_{i-1}}{h_i}\tau_i$$

Therefore

$$M_i = \frac{-M_{i+1}}{\frac{h_{i-1}}{h_i}\rho_i + 2\left\{1+\frac{h_{i-1}}{h_i}\right\}} + \frac{d - \frac{h_{i-1}}{h_i}\tau_i}{\frac{h_{i-1}}{h_i}\rho_i + 2\left\{1+\frac{h_{i-1}}{h_i}\right\}} \qquad (4.7)$$

This has the same form as equation (4.6) hence

$$\rho_{i+1} = \frac{-1}{\frac{h_{i-1}}{h_i}\rho_i + 2\left\{1 + \frac{h_{i-1}}{h_i}\right\}}$$

and

$$\tau_{i+1} = \frac{d_i - \frac{h_{i-1}}{h_i}\tau_i}{\frac{h_{i-1}}{h_i}\rho_i + 2\left(1 + \frac{h_{i-1}}{h_i}\right)}$$

If it can be proved that no denominator vanishes this gives a simple recursion for computing ρ_i and τ_i ($i = 2,3,\ldots,n$). Then starting with $M_n = 0$ equation (4.6) may be used to calculate M_i in the order (n-1, n-2, ...,2).

To prove $\frac{h_{i-1}}{h_i}\rho_i + 2\left(1+\frac{h_{i-1}}{h_i}\right) \neq 0$ for all i

Clearly $|\rho_2| < 1$ If $|\rho_i| < 1$ then

$$\left|\frac{h_{i-1}}{h_i}\rho_i + 2\left(1+\frac{h_{i-1}}{h_i}\right)\right| = \left|\frac{h_{i-1}}{h_i}(\rho_i+2)+2\right|$$

$$\geq \left|\frac{h_{i-1}}{h_i} + 2\right| > 2.$$

Therefore equation (4.7) holds and the recursion expression for the M_s is finite.

4.4 *Parametric Cubic Spline*

It has been shown that for a variable t and its corresponding dependant variable F(t) that a smooth curve may be generated to interpolate the fixed points.

If the variable t is assumed to be the variable x and F(t)

assumed to be y (x and y being the cartesian plane co-ordinates), then for any x value using Splines $S_i(x)$ may be found. But this is of no direct avail in representing a multi-valued function of x, eg. a closed curve, or a curve that doubles back on itself or has double or multiple points or if it is an open curve with very large slope, $dy/dx \to \infty$ at some point in its range. However such functions $y = F(x)$ can be represented in parametric form.

$$y = F(t) \; ; \quad x = G(t)$$

where t is a parameter with values in a certain interval; hence the two-dimensional parametric natural cubic spline is

$$F_i(t) = y = a_i t^3 + b_i t^2 + c_i t + d_i \qquad \text{(a)}$$

$$G_i(t) = x = e_i t^3 + f_i t^3 + g_i t + h_i \qquad \text{(b)} \qquad (4.8)$$

This produces two splines in t and the previous theory of splines can be applied to each, considering nodes in the interval of t which are strictly increasing in value.

Here $$dy/dx = \frac{dy/dt}{dx/dt}$$

Values of t for which $dx/dt = 0$ correspond to where the slope is infinite. In this type of cubic spline one can find in general, three separate values of t which give the same value of x and of course in general three different y values allowing it to represent curves which form loops or even double loops. It has been specified that t must be strictly increasing between (x_1, y_1) and

$x_n, y_n)$, that is, on the curve in the x, y plane if t takes the value T_i at the point (x_i, y_i) and taken the value t at the point (x,y) and takes the value T_{i+1} at the point (x_{i+1}, y_{i+1}) then $T_i < T_{i+1}$. This means that in the (t,x) plane and (t,y) plane x and y are single valued functions of t. If this parameter t is considered as the distance along the curve then the resulting cubics in t, for x and y give the curve in the (x,y) plane of that formed by the spline. If t is the distance from the point (x_1, y_1) to the point (x,y) on the spline along the spline then the spline may be represented by equations (4.8) (a) and (b). The values T_i at the point (x_i, y_i) are not known and must be estimated.

4.4.1 *Estimation of Curve longth*

As the parameter t is considered the distance along the curve, then the curve length must be estimated before the curve is found. The procedure used is to write a cubic polynomial of the form

$$t = ax^3 + bx^2 + cx + d \qquad (4.9)$$

for each interval $|x_i, x_{i+1}|$ and evaluate the integral

$$L = \int_{xi}^{x_{i+1}} \{1 + (dy/dx)^2\}^{\frac{1}{2}} dx$$

The integration is formed numerically using Gaussian quadrature with four Gauss points.

The curve must be well behaved that is θ_i or θ_{i+1} must not equal 90^o and $|\theta_i - \theta_{i+1}| < 180^o$; if these two conditions

are not satisfied the line must be rotated towards the horizontal before integration.

The resulting lengths for each interval are added to give the length of the whole curve. Obviously as this is an estimated length, the error accumulates as the curve length increases. When the spline is found using these estimated lengths, the lengths are re-calculated and by an iterative process an improved curve length may be found hence giving a better fit to the locus of the knots.

4.4.2 *Estimation of Slope at node points*

An alogrithm to provide values for the slope at the point P_i can be developed by finding the equation of a curve through P_i and several adjacent points and by taking the derivative of the curve at P_i, McConologue (1970). The slope at each node is needed to determine the constants a, b, c and d in equation (4.9).

To find these four unknowns, four equations are needed within the interval (x_i, x_{i+1}).

These are

$$y_i = ax_i^3 + bx_i^2 + cx_i + d \qquad (4.10)$$

$$y_{i+1} = ax_{i+1}^3 + bx_{i+1}^2 + cx_{i+1} + d$$

$$\tan\theta_i = 3ax_i^2 + 2bx_i + c$$

$$\tan\theta_{i+1} = 3ax_{i+1}^2 + 2bx_{i+1} + c$$

The function to be differentiated is in parametric form to be compatible with the parametric spline. The method used is to pass a parabola through three successive points p_{i-1}, p_i, p_{i+1}, the x and y co-ordinates being given independently in terms of a parameter u. Such a parabola is not unique, but values for the slope acceptable over a wide range of applications is obtained by writing x and y independently as Lagrangian interpolating polynomials in u, where x and y have the values x_{i-1} and y_{i-1} at $u = D_{i-1}$, x_i, y_i at $u = 0$ and x_{i+1}, y_{i+1} at $u = D_i$ where

$$D_i = \{(\Delta x_i)^2 + (\Delta y_i)^2\}^{\frac{1}{2}} \qquad (4.11)$$

$$\Delta x_i = x_{i+1} - x_i$$

$$\Delta y_i = y_{i+1} - y_i$$

Differentiating these equations and simplifying gives the following equations for the slope at any point p_r:

$$\begin{aligned} \text{Cos}\theta_r &= C_r/N_r \\ \text{Sin}\theta_r &= S_r/N_r \end{aligned} \qquad (4.12)$$

where

$$\begin{aligned} C_r &= \Delta x_{i-1}\alpha_r + \Delta x_i \beta_r \\ S_r &= \Delta y_{i-1}\alpha_r + \Delta y_i \beta_r \\ N_r &= \left| c^2{}_r + S^2{}_r \right|^{\frac{1}{2}} \\ \text{slope} = T_r &= \frac{S_r}{C_r} \end{aligned} \qquad (4.13)$$

On the assumption that the positive direction along the curve is from P_{i-1} to P_{i+1}.

$$\alpha_r = D_i(2D_{i-1} + D_i),\ D^2{}_i \text{ and } -D^2{}_i \text{ for}$$

$$r = i-1,\ i, \text{ and } i+1 \text{ respectively}$$

and

$$\beta_r = D^2{}_{i-1},\ D^2{}_{i-1},\ D_{i-1}(D_{i-1} + 2D_i) \text{ for}$$

$$r = i-1,\ i \text{ and } i+1 \text{ respectively.}$$

The form r = i is normally used where possible, those for r = i-1 and r = i+1 being used for the beginning and end of an open curve or at points on an open or closed curve where there are cusps and other discontinuities in the derivative. However the method used here in obtaining slopes at node 1 and node n is to generate nodes 0 and n+1 by taking x_o as $x_1 - (x_2-x_1)$ and x_{n+1} as $x_n + (x_n-x_{n-1})$ and by spline interpolation finding the corresponding y values i.e. y_o and y_{n+1}. Hence nodes 1 and n are internal nodes thus the form r = i is used.

4.4.3 *Interpolating Intermediate Points*

At the nodes the value of the parameter t coincides with the distance from an arbitrary point (x_1,y_1). It is not true that an intermediate value of the parameter t represents a point that has the same value for the distance to the point, for if distance $\{(x_1,y_1), (x,y)\}$ equals the distance along spline from (x_1,y_1) to (x,y) and if distance $\{(x_1,y_1), (x_1,y_1)\} = s_i$ and (x_i,y_i) is a node point with the parameter value $t = t_i$

$$\text{then } t_i = s_i$$

But if distance $\{(x_1,y_1).\ (x,y)\}$ is s and (x,y) is some point on the spline with parameter value $t = T \neq t_i$ then $T = s$ is not necessarily true. However there is necessarily continuity of the parameter t and distance s and the parameter values are coincident with the distance values at the nodes. From this it is known between which two nodes a given value of the distance s lies, the bounds between which the associated parameter value T will lie can be found.

$$\text{If } s_i < s < s_{i+1} \text{ then } t < T < t_{i+1}$$

In terms of the parameter t in equations (4.8) (a) and (b) the distance along the spline is given by

$$s = t_i + \int_{ti}^{T} \{F_i^1(t)\}^2 + \{G_i^1(t)^2\}^{\frac{1}{2}} dt \qquad (4.14)$$

The numerical evaluation of this expression for the unknown T yields the associated parameter of the distance s, and hence x and y coordinates for any point on the curve.

The procedure is illustrated schematically in the mapping shown in Fig. 4.3.

FIGURE 4.3: *Parametric Mapping of plane curve*

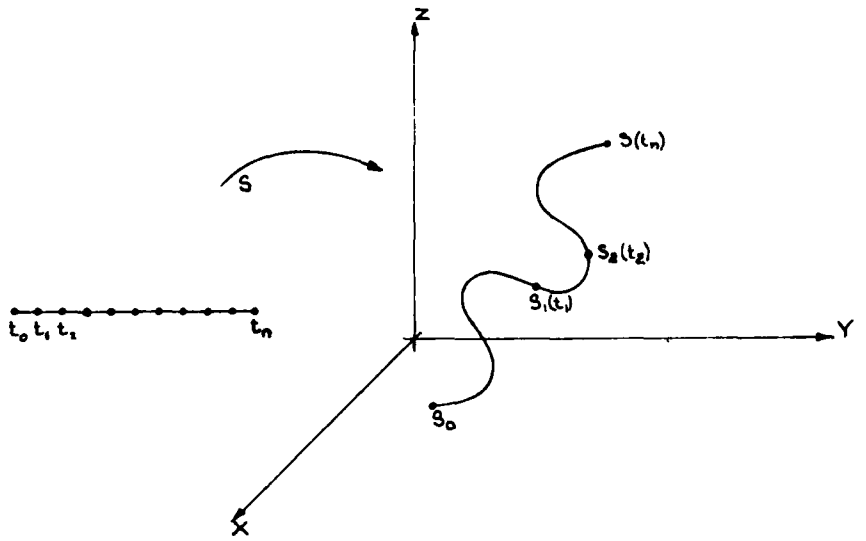

4.5 *Data Input*

A computer program based on foregoing theory was written in Fortran IV for interpolating flow nets by parametric cubic splines (O'Laoide, 1979). The computer program is structured to compute x and y co-ordinates for given lengths along a curve. It also computes x co-ordinates for given y co-ordinates and calculates the slope of the curve at a given x co-ordinate.

The number of nodes with their co-ordinates must be read in, and when the number of nodes is given as zero the program is terminated.

The program has six input types and are as follows:

Two pointers, denoted by L and M, enable selection of a set of options as follows:

L=1 a length is read in and the corresponding x and y co-ordinates are calculated

L=2 a length of increment is read in with an upper and lower bound. The x and y co-ordinates for each incremental length are calculated

L=3 an x co-ordinate is read in and its corresponding y co-ordinate is calculated

L=4 an x co-ordinate increment is read in with an upper and lower bound. The y co-ordinates for each incremental x co-ordinate are calculated

L=5 an x co-ordinate is read in and the slope of the curve at that co-ordinate is calculated

L=6 an x co-ordinate increment is read in with an upper and lower bound, and the corresponding slopes within the range are calculated.

When M = 0, for L = 1,2,3 and 4 the slopes corresponding to the x co-ordinates will also be calculated. When M = 2 a cumulative chord length is read in and the corresponding x and y coordinates are calculated.

4.6 *Applications of Cubic Spline in Harmonic Analysis*

Interpolation of Contour Intervals

Normally a spline is viewed as an ordinary function which gives the value of the dependent variable for a prescribed value of the independent variable (in a closed interval). In what follows it is demonstrated that a

reverse process can be implemented whereby the dependent variable can take on prescribed values and the original independent variable can be treated as a dependent variable. This transition provides a means of plotting contours for monotonic functions and in particular solutions of Lapace's equation with coordinates (x,y, Ø) say, where Ø is the potential.

To map the contours we require ordinates at stations along a grid line where the ordinates differ by a preset value i.e. the contour interval. A cross-section on any grid line will normally have contour ordinates at irregularly spaced distances from the origin of the cross section. Each contour ordinate t_c is located at a root of the equation

$$S_i(\phi) - t_c = 0 \qquad 4.15$$

where $S_i(\phi)$ is the spline function representing $f(\phi)$ through the knots in the interval $|x_i, x_i + 1|$ or in interval $|y_i, y_i + 1|$.

The roots of the Equation 4.15 can be determined with any degree of accuracy by repeated application of the Newton-Raphson formula, provided that there is no local extremum of the function in the neighbourhood of a root. This condition is satisfied by all harmonic functions if sources and sinks are isolated in the physical problem.

Reverting to the notation of the parametric cubic spline Equation 4.2 and 4.15 are written in the form:

$$S_i(t) - t_c = a_i t^3 + b_i t^2 + c_i t + d_i - t_c = 0$$

where

$$a_i = \frac{1}{6h_i}(M_{i+1} - M_i)$$

$$b_i = \frac{1}{2h_i}(M_i t_{i+1} - M_{i+1} t_i)$$

$$c_i = \frac{1}{2h_i}(M_{i+1} t_i^2 - M_i t_{i+1}^2) - \frac{hi}{3}(M_{i+1} - M_i)$$

$$d_i = \frac{1}{h_i}\left|F(t_i) - \frac{M_i h_i^2}{6}\right| t_{i+1} - \frac{1}{h_i}\left|F) t_{i+1}) - \frac{M_{i+1} h_i^2}{6}\right| t_i + \frac{i}{6h_i}(M_i t_{i+1}^3 - M_{i+i} t_i^3)$$

$$h_i = t_{i+1} - t_i \qquad 4.16$$

By applying the Newton-Raphson formula

$$t_{n+1} = t_n - \frac{S_i(t_n)}{S_i'(t_n)} \qquad 4.17$$

n = iteration number

the first approximation to a root within the interval $|t_i, t_{i+1}|$ is conveniently derived by letting $t_n = t_i$, or alternatively $t_n = t_{i+1}$. The roots for a given value t_c will be available on lines parallel to both x and y coordinate axis by simple looping. However it is necessary to sort the array of roots to ensure that those roots in close proximity are grouped together for machine plotting of the contour ordinate as a sequential curve.

Transformation of Boundary Conditions

To fully avail of the properties of harmonic functions

an automatic means of converting boundary conditions is required. The Dirichlet problem is one of finding a function u to satisfy

$$\nabla^2 u = 0 \qquad (u)_s = f \tag{4.18}$$

where f is a function of position on the boundary s and ∇^2 is the Laplacian operator.

The Neumann problem is that of finding a function u to satisfy

$$\nabla^2 u = 0 \qquad \left(\frac{\delta u}{\delta n}\right)_s = g \tag{4.19}$$

where g is a given function of position on the boundary s and $\frac{\delta u}{\delta n}$ is the normal derivative outward from the region considered. By using the Cauchy-Riemann equations either the Dirichlet or the Neumann boundary value problems may be transformed into the other.

On the boundary s the Cauchy-Riemann equations imply

$$\frac{\delta u}{\delta s} = - \frac{\delta v}{\delta n}$$

where $\frac{\delta u}{\delta s}$ is the tangential derivative of the function u in the positive sense (region of analyticity on the left i.e. counterclockwise circulation) along the boundary, and $\frac{\delta v}{\delta n}$ is the normal derivative of the conjugate function outward from the region. From analyticity requirements the integral of $\frac{\delta u}{\delta s}$ around a complete boundary must be zero (i.e. property of perfect differential) so the Neumann problem $\left(\frac{\delta v}{\delta n}\right) = g$ has no solution unless g satisfies

$$\oint_s g \, ds = 0 \qquad 4.20$$

The cubic spline provides a means of checking boundary conditions via the first derivatives at the knots.

4.7 *REPRESENTATION OF SPLINE FUNCTIONS BY TRUNCATED POWER SERIES*

The cubic spline enforces C^2 - continuity at the knots and hence gives an adequate representation of the mean stress contours of the harmonic problem. On the other hand the solution of the biharmonic equation demands C^4 - continuity, therefore for completeness reference is made to the truncated power series representation known as the Schoenberg-Whitney formula as follows:

$$S(x) = P(x) + \sum_{J=1}^{n} C_J \, (x - x_j)_+^m$$

where $P \in P$

and $(x - x_j)_+^m = 0 \qquad$ If $x \leq x_J$

$$= x - x_j \text{ if } x > x_j \qquad 4.21$$

P_m denotes the class of polynomials of degree m or less, and c_1----c_n are the unknown constants.

In beharmonic analysis the appropriate spline is:

$$S(x) = a_o + a_1 x + a_2 x^2 + a_3 x^3 + a_4 x^4 + a_5 x^5 +$$

$$\sum_{J=1}^{n} C_J (x - x_J)_+^5 \qquad 4.22$$

where the interval is divided into (n+1) equal length segments. There are (n + 6) unknown constants in the quintic spline which are evaluated by collocation at the n knots (x_1, x_2----x_n) and at the end points x_o and x_{n+1} by using two boundary conditions at each end of the interval. The Schoenberg-Whitney formula produces a cubic spline if m = 3 and the set of polynomials P is equal to or less than P_m. The resulting representation is an aggregate of B-splines.

CHAPTER 5

HARMONIC ANALYSIS OF STRESS FIELDS

5.1 *Finite Difference Approximations*

As mentioned earlier the solution of Laplace's Equation gives the distribution of mean stress within a two dimensional domain provided that precise boundary conditions can be enforced. In this Chapter the question of extending harmonic analysis to axisymmetric problems is investigated. The objective is to prescribe sufficient boundary conditions to enable a numerical solution. The choice of finite difference, finite element or boundary element techniques is one of personal preference; the three methods are equally applicable in the majority of cases but the FEM has some special advantages for non-homogeneous problems, Fenner (1975) Frind (1977) Huebner (1975) and several other authors. In stress analysis these methods yield data for plotting the contours of mean stress if Dirichlet-type conditions are imposed on the boundaries (Neumann-type conditions may be more easily specified in other areas such as fluid mechanics). Where the analysis is confined to a subdomain of a continuum as in the axisymmetric flow problem the specification of boundary conditions is identical for any one of the numerical methods (finite differences, fininte elements or boundary elements). The values of the mean normal stress must be prescribed at the external nodes of the discretised domain. The finite difference method is adopted herein because it simplifies the numerical calculations if the domain is assumed to consist of a homogeneous and isotropic half space (where it is possible to specify a constant grid interval on mutually perpendicular coordinate axis).

The governing differential equations for axially symmetric stress distribution take the form, Timosnenko and Goodier (1951);

$$\nabla^2\sigma_r - \frac{2}{r^2}(\sigma_r-\sigma_\theta) + \frac{1}{1+\nu}\frac{\delta^2\Theta}{\delta r^2} = 0 \qquad \text{(a)}$$

$$\nabla^2\sigma_\theta + \frac{2}{r^2}(\sigma_r-\sigma_\theta) + \frac{1}{1+\nu}\frac{1}{r}\frac{\delta\Theta}{\delta r} = 0 \qquad \text{(b)}$$

$$\nabla^2\sigma_z + \frac{1}{1+\nu}\frac{\delta^2\Theta}{\delta z^2} = 0 \qquad \text{(c)}$$

$$\nabla^2\tau_{rz} - \frac{1}{r^2}\tau_r + \frac{1}{1+\nu}\frac{\delta^2\Theta}{\delta r\delta z} = 0 \qquad \text{(d)} \qquad 5.1$$

where Θ denotes the mean normal stress multiplied by a factor of three, and the remaining terms are in the usual notation for cylindrical coordinates. By adding (a) (b) and (c) of above set it can be shown that the governing equations reduce to the following expression:

$$\frac{\delta^2\Theta}{\delta r^2} + \frac{1}{r}\frac{\delta\Theta}{\delta r} + \frac{\delta^2\Theta}{\delta z^2} = 0 \qquad 5.2$$

where Θ can be interpreted as a stress potential in the absence of body forces.

5.2 *Boundary Conditions in Terms of Mean Stresses*

Dirichlet Boundary Value Problem The stress distribution in the elasto-isotropic medium for a uniformly loaded circular area can be calculated by means of the Boussinesq solution for a concentrated load, the principle of superposition and Maxwell's reciprocal theorem. The stresses in the vertical and radial

directions are given by the expressions; Timosheuko and Goodier (1951):

$$\sigma_r = -\frac{P}{2\pi}\left\{\frac{3r^2 z}{(r^2+z^2)^{5/2}} - (1-2\nu)\left[\frac{1}{r^2} - \frac{z}{r^2(r^2+z^2)^{1/2}}\right]\right\}$$

$$\sigma_\theta = -\frac{P}{2\pi}(1-2\nu)\left\{\frac{1}{r^2} - \frac{z}{r^2(r^2+z^2)^{1/2}} - \frac{z}{(r^2+z^2)^{3/2}}\right\}$$

$$\sigma_z = -\frac{3P}{2\pi}\left[\frac{z^3}{(r^2+z^2)^{5/2}}\right]$$

$$\tau_{rz} = -\frac{3P}{2\pi}\left[\frac{rz^2}{(r^2+z^2)^{5/2}}\right]$$

$$\Theta = \sigma_r + \sigma_\theta + \sigma_z = \sigma_x + \sigma_y + \sigma_z \qquad 5.3$$

where P is a concentrated vertical load and r, z, θ are the ordinates of cylindrical coordinate system.

The stress components can be found directly but the calculations are cumbersome, Harr (1966) Jumikis (1969) Ahlvin and Ulery (1962). The direct methods generally reduce to the evaluation of elliptic intergals which are not easily handled in a computer program. In this section an approximate method based on superposition is presented.

The uniform loading, or other continuous distribution, is replaced by equivalent line loads on annular rings. The method involves summing the stresses generated at the boundary nodes by point loads on differential arc lengths.

Let P denote the line load per unit length of annular ring as shown in Fig. 5.1 and let W denote the total load on the annular ring.

Then $P = W/2\pi r_a$ where r_a is the mean radius of ring and the distance to the boundary of finite difference mesh is given by :-

$$d = (r^2+h^2-2rh\ \cos\theta)^{\frac{1}{2}}$$

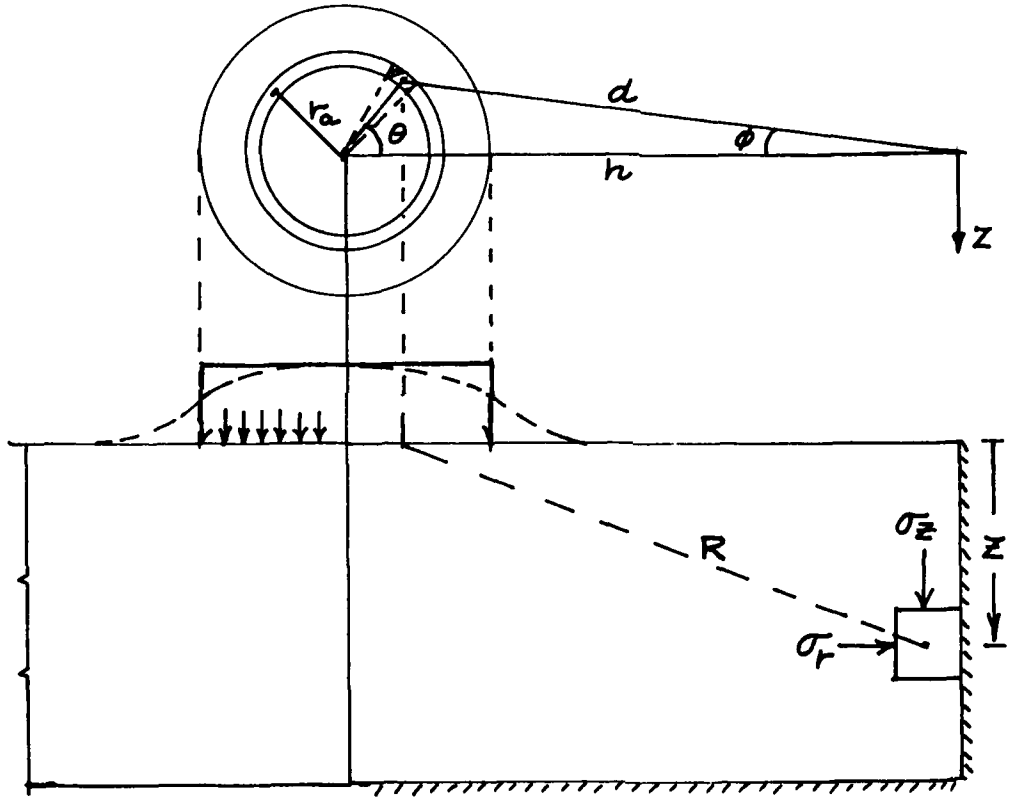

5.1 Normal Load over Circular Area

The stresses on the edges of any diametral plane passing through the axis of symmetry are given by the expressions:

$$\sigma_r = -\frac{P}{2\pi}\left\{\left[\frac{3zd^2}{R^5} - \frac{1-2\nu}{R(R+z)}\right]\cos^2\phi - (1-2\nu)\left[\frac{1}{R(R+z)} - \frac{z}{R^3}\right]\sin^2\phi\right\}$$

$$\sigma_\theta = -\frac{P}{2\pi}\left\{\left[\frac{3zd^2}{R^5} - \frac{1-2\nu}{R(R+z)}\right]\sin^2\phi - (1-2\nu)\left[\frac{1}{R(R+z)} - \frac{z}{R^3}\right]\cos^2\phi\right\}$$

$$\sigma_z = -\frac{3P}{2\pi}\frac{z^3}{R^5} \quad : \quad \tau_{rz} = -\frac{3P}{2\pi}\frac{z^2 d}{R^5} \qquad 5.4$$

where $R^2 = z^2 + d^2$

$$\phi = \text{Arc Cos} + \frac{d^2+h^2-r^2}{2dh}$$

and $0 \leq \theta \leq 2\pi$; $0 < \phi \leq \pi/4$

Because of symmetry the superposition of stresses is performed in the range $0 \leq \theta \leq \pi$ with small increments of θ corresponding to unit length of arc for each annular ring. Nodes on the axis of symmetry are treated separately because the stresses can be related to total load W on the rings. The stress components on the axis of symmetry for uniform pressure on circular contact area are given by the expressions

$$\sigma_r = \sigma_\theta = -\frac{q_o}{2}\left[(1-2\nu) - \frac{2(1+\nu)z}{(a^2+z^2)^{1/2}} + \frac{z^3}{(a^2+z^2)^{3/2}}\right]$$

$$\sigma_z = -q_o\left[1 - \frac{z^3}{(a^2+z^2)^{3/2}}\right] \qquad 5.5$$

where q_o denotes the uniform loading distribution over the area of the circle of radius a.

5.3 *Boundary Tractions*

Discontinuities in surface tractions such as occur at the extremities of a uniformly distributed load are detrimental in a finite difference analysis. Smoothing by equivalent continuous functions of the load distribution seems imperative. A uniform load distribution over part of the boundary is reasonably approximated by the expression

$$q = q_o \operatorname{Sech}^2 \frac{\rho}{a}$$

$$0 \leq \rho \leq h$$

because the definite integral of the function converges within a short distance of the edge of the uniformly loaded area (as shown in the following tabulation) i.e.

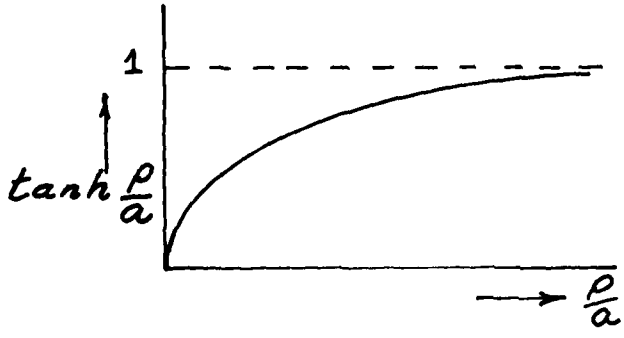

$$\int \operatorname{Sech}^2 \frac{\rho}{a}\, d\left(\frac{\rho}{a}\right) = \tanh \frac{\rho}{a}$$

TABLE V-1: *Approximating Function for Symmetrical Square Wave*

$\frac{\rho}{a}$	Sech $(\frac{\rho}{a})$	Sech^2 $(\frac{\rho}{a})$	tanh $(\frac{\rho}{a})$
0.0	1.0000	1.0000	0.0000
0.2	0.9803	0.9610	0.1974
0.4	0.9250	0.8556	0.3799
0.6	0.8435	0.7115	0.5370
0.8	0.7477	0.5591	0.6640
1.0	0.6480	0.4199	0.7616
1.2	0.5523	0.3050	0.8336
1.4	0.4649	0.2161	0.8853
1.6	0.3880	0.1505	0.9217
1.8	0.3218	0.1036	0.9468
2.0	0.2658	0.0706	0.9640
2.4	0.1800	0.0324	0.9837
3.0	0.0993	0.0093	0.9950

Accelerated convergence to a uniform load distribution can be achieved by assuming weighting factors in the range 1 to 2; one such factor leads to the expression;

$$q = q_o \text{ Sech}^2 \sqrt{2} \frac{\rho}{a} \qquad 5.6$$

where q_o is the amplitude of the uniformly distributed load and ρ denotes distance from axis of symmetry. The potential function on free boundary is $\theta \equiv -q$.

The Dirichlet conditions of the original problem are thusly replaced by equivalent distributions of mean normal stresses on the boundaries with nodal values taking on the ordinate values of this distribution via a superposition technique.

5.4 Finite Difference Operator

Let the differential Equation 5.2

$$\frac{\delta^2\Theta}{\delta r^2} + \frac{1}{r}\frac{\delta\Theta}{\delta r} + \frac{\delta^2\Theta}{\delta z^2} = 0$$

be represented by difference equations

$$\left(\frac{1}{\lambda_n^2} - \frac{1}{2r\lambda_h}\right)\Theta_{i,j-1} - 2\left(\frac{1}{\lambda_h^2} + \frac{1}{\lambda_v^2}\right)\Theta_{i,j}$$

$$+ \left(\frac{1}{\lambda_h^2} + \frac{1}{2r\lambda_n}\right)\Theta_{i,j+1} + \frac{1}{\lambda_v^2}\Theta_{i+1,j} + \frac{1}{\lambda_v^2}\Theta_{i-1,j} = 0$$

On the axis of symmetry

$$\frac{\delta\Theta}{\delta r} = 0$$

By differentiating the numerator and denominator (as in L'Hospital's Rule)

$$2\frac{\delta^2\Theta}{\delta r^2} + \frac{\delta^2\Theta}{\delta z^2} = 0$$

Hence on the axis

$$\frac{2}{\lambda_h^2}(\Theta_{i,j-1} - 2\Theta_{i,j} + \Theta_{i,j+1}) + \frac{1}{\lambda_v^2}(\Theta_{i+1,j} - 2\Theta_{i,j} + \Theta_{i-1,j}) = 0 \qquad 5.7$$

where the nodes and intervals are shown in Fig. 5.2

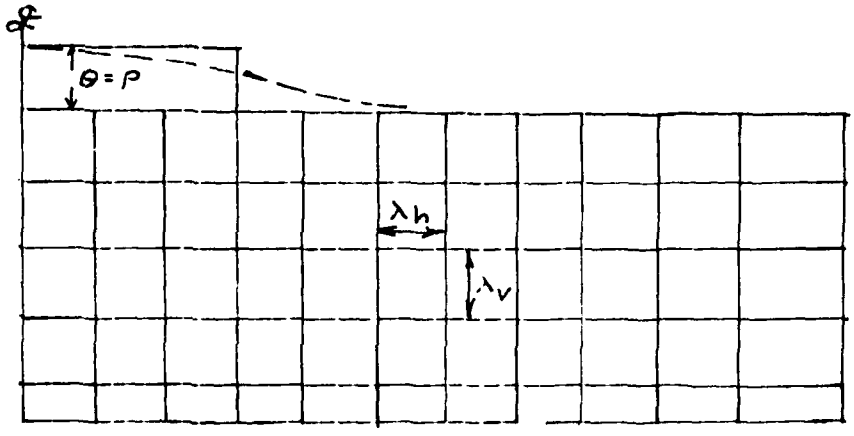

Fig. 5.2 Finite Difference Mesh

Neumann Boundary Value Problem The Equation 5.2 for the potential function in terms of mean stress is analagous to the equation of velocity potential in fluid mechanics. The starting point for its derivation is the Continuity Equation of an incompressible fluid.

$$\frac{\delta V_r}{\delta r} + \frac{V_r}{r} + \frac{\delta V_z}{\delta z} = 0$$

$$V_r = \frac{\delta \Phi}{\delta r}, \quad V_z = \frac{\delta \Phi}{\delta z}$$

which yields

$$\frac{\delta^2 \Phi}{\delta r^2} + \frac{1}{r}\frac{\delta \Phi}{\delta r} + \frac{\delta^2 \Phi}{\delta z^2} = 0 \qquad 5.8$$

where V denotes velocity and Φ velocity potential.

By specifying boundary conditions based on the first derivative of Φ the solution for the stream lines is

obtained. The Neumann problem is posed by taking as the Continuity Equation the expression

$$\frac{\delta V_r}{\delta z} - \frac{\delta V_z}{\delta r} = 0$$

$$V_r = \frac{1}{r}\frac{\delta \psi}{\delta z}, \quad V_z = -\frac{1}{r}\frac{\delta \psi}{\delta r}$$

which yields

$$\frac{\delta^2 \psi}{\delta r^2} + \frac{1}{r}\frac{\delta \psi}{\delta r} + \frac{\delta^2 \psi}{\delta z^2} = 0 \qquad 5.9$$

where the boundary conditions are those discussed in Chapter 4. The solution of the Neumann problem can be extracted to within an arbitrary constant throughout the domain. There are sufficient data for contouring lines of constant ψ, and in fact the same solution routine can be used for finding ϕ and ψ simply by inserting a linking subroutine to generate the ψ values at the nodes of the boundary. An interesting variant of this approach has been reported for the problem of seepage through an earth dam, Shaug and Bruch (1976). However, for the stress distribution problem the Neumann conditions pertain to strain energy density which are difficult to prescribe. Hence an alternative method is required for finding orthogonal trajectories to the mean stress contours.

The problem of orthogonal slip-line fields is extensively covered in applications of plasticity theory, hence as a preliminary to the present author's approach to potential field problems a brief outline of methods employed in plastic analysis is included in the next section.

5.5 *Slip-Line Fields in Plasticity Theory*

Method of Characteristics

The theory of the ideal plastic solid yields differential equations for solution of the geometrical constraints on the slip lines. For the case of plane strain the governing differential equation is derived on the following assumptions:-

1. the shear stress has a yield value k which is induced at every point on a slip line,
2. the equilibrium equations are identical to those of elasticity theory,
3. the direct stress normal to the slip line is the mean stress devoted by
4. the geometrical constraints on the slip lines can be referred to Cartesian coordinates with the angle subtended by normal to the plane of maximum shear and the x-axis the identifying parameter (denoted by α) as depicted in Fig. 5.3.

Consider a homogeneous weightless material in a state of limiting equilibrium. The equilibrium equations are given by the expressions, Unksov (1961):-

$$\frac{\delta \sigma_x}{\delta x} + \frac{\delta \tau_{xy}}{\delta y} = 0$$

$$\frac{\delta \tau_{xy}}{\delta x} + \frac{\delta \sigma_y}{\delta y} = 0 \qquad 5.10$$

and the stress state in terms of σ and k is as follows:-

$$\begin{aligned} \sigma_x &= \sigma + k \text{ Sin } 2\alpha \\ \sigma_y &= \sigma - k \text{ Sin } 2\alpha \\ \tau_{xy} &= - k \text{ Cos } 2\alpha \end{aligned} \qquad 5.11$$

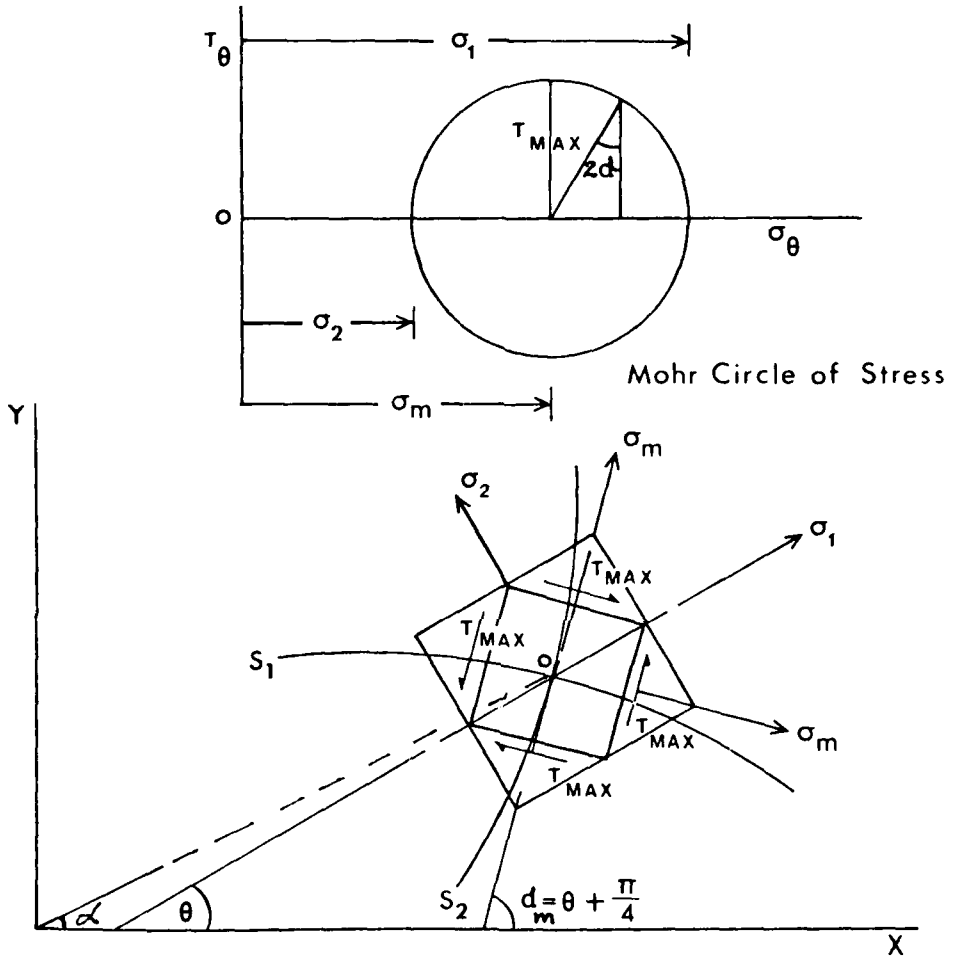

Fig. 5.3 Slip Lines S1, S2 and Normal Stresses Directions at Point O.

By substituting the expressions 5.11 into 5.10 the equilibrium equations in terms of the mean stress become:

$$\frac{\delta\sigma}{\delta x} + 2k(\text{Cos } 2\alpha \frac{\delta\alpha}{\delta x} + \text{Sin } 2\alpha \frac{\delta\alpha}{\delta y}) = 0$$

$$\frac{\delta\sigma}{\delta y} - 2k(\text{Cos } 2\alpha \frac{\delta\alpha}{\delta y} - \text{Sin } 2\alpha \frac{\delta\alpha}{\delta x}) = 0 \qquad 5.12$$

On eliminating σ, by differentiating the first of 5.11 with respect to x and the second to y the single differential equation is obtained by subtraction viz.

$$-\frac{\delta^2\alpha}{\delta x^2} + 2 \text{ Cot } 2\alpha \frac{\delta^2\alpha}{\delta x \delta y} + \frac{\delta^2\alpha}{\delta y^2} - 4 \frac{\delta\alpha}{\delta x} \cdot \frac{\delta\alpha}{\delta y} +$$

$$2 \text{ Cot } \alpha \left[(\frac{\delta\alpha}{\delta y})^2 - (\frac{\delta\alpha}{\delta x})^2\right] = 0 \qquad 5.13$$

By the theory of differential equation the so-called characteristic equation for 5.12 is given by

$$-dy^2 - 2 \text{ Cot } 2\alpha \, dx \, dy + dx^2 = 0 \qquad 5.14$$

The roots of equation 5.13 are both real i.e. the equation 5.12 is hyperbolic, and lead to the solution for the characteristic directions as follows:

$$(\frac{dy}{dx})_1 = -\text{Cot } 2\alpha + (\text{Cot}^2 2\alpha + 1)^{\frac{1}{2}}$$

$$= -\frac{\text{Cos } 2\alpha}{\text{Sin } 2\alpha} + \frac{1}{\text{Sin } 2\alpha} = \tan\alpha$$

$$(\frac{dy}{dx})_2 = -\text{Cot } 2\alpha - (\text{Cot}^2 2\alpha + 1)^{\frac{1}{2}} = -\text{Cot}\alpha \qquad 5.15$$

It follows that the tangents to the slip lines at any point form angles with the x-axis which are given by the equalities

AD-A118 234 TRINITY COLL DUBLIN (IRELAND) DEPT OF CIVIL ENGINEERING F/G 20/11
NUMERICAL METHODS FOR CREEP ANALYSIS IN GEOTECHNICAL PROBLEMS.(U)
DEC 81 T E GLYNN DAERO-76-6-063

UNCLASSIFIED NL

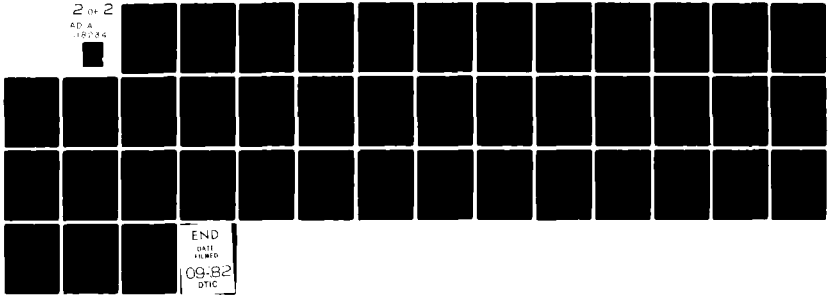

$$\frac{dy}{dx} = \tan \alpha \ , \ \frac{dy}{dx} = - \text{Cot } \alpha$$

In other words, the characteristics coincide with the slip lines and form an orthogonal system; the characteristics cut a free surface at a constant angle of 45^{o}. Thus the geometrical constraint is that the slip lines should form an orthogonal mesh within the solution domain.

Because the foregoing equation is of the hyperbolic type it is theoretically feasible to propagate the stress field solution by integration along the characteristics, Harr (1966) pp 24 to 253. However, the procedure is difficult to implement because it requires much physical interpretation as demonstrated by Sokolovsky and other researchers. On the other hand, purely geometrical techniques, such as Prager's graphical method, is favoured for intricate problems.

Matrix Technique for Constructing Slip Lines

A matrix analysis for constructing slip-line solutions has been reported by Dewhurst and Collins (1973). The procedure is based on a power series representation of the solution to the governing equations first used by Ewing (1967). By starting with base slip-lines with radii of curvature $R_o(\alpha)$ and $S_o(\beta)$ the initial curvatures are expanded as power series in the angular coordinate.

$$R_o(\alpha) = \sum_{n=o}^{\infty} a_n \frac{\alpha^n}{n!} \ , S_o(\beta) = \sum_{n=o}^{\infty} b_n \frac{\beta^n}{n!} \qquad 5.15$$

By introducing Mikhlin co-ordinates $(\bar{x},\bar{y})$ it can be shown that the relationship between the coefficients in power series expansions of these co-ordinates and of the radii of curvature is as follows:

$$R(\alpha) = \sum_{n=o}^{\infty} r_n \frac{\theta^n}{n!}$$

$$\bar{x}(\theta) = \sum_{n=o}^{\infty} t_n \frac{\theta^n}{n!}$$

$$\bar{y}(\theta) = \mp \sum_{n=o}^{\infty} t_n \frac{\theta^{n+1}}{(n+1)!}$$

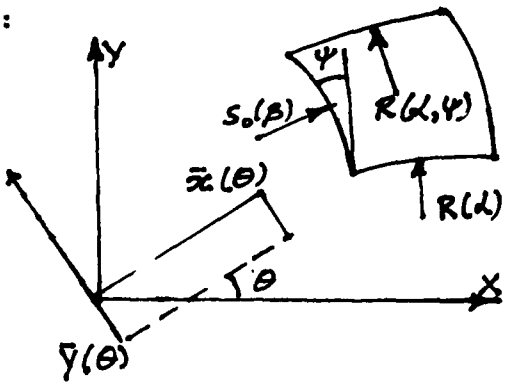

and the t_n's are given by the recurrence relation

$$t_{n+1} - t_{n-1} = |r_n|, \; t_o = 0, \; t_1 = |r_o|$$

where the terms are defined in the original paper. The subsequent matrix formulation leads to a general method for 'marching out' the solution of plane strain rigid perfect-plasticity problems.*

Of course the finite element method has made an impact in plasticity problems. Zienkiewicz and Godbole (1975). These authors compare various methods for treating viscous incompressible flow with special reference to Non-Newtonian (Plastic) fluids.

Essentially all the methods aspire to constructing the α-β net which gives a graphical picture of the deformation mode.

---

* Program listing in FORTRAN is appended to the paper, Dewhurst and Collins (1973).

5.6 *Orthogonal Trajectories to Countours of Mean Stresses: A New Numerical Method.*

In the course of this study it became evident that a technique more versatile than that presented in Chapter 3 is needed. In particular if the special attributes of parametric splines are to be exploited for plotting trajectories of mean and shear stresses a solution format analogous to the matrix method for plasticity is a desirable goal. Apart from applications of complex variable theory and trial and error sketching of flow nets no techniques emerged from an extensive literature search. The present author expended considerable effort to simply find a framework for the problem, because there are a number of possible formulations, for instance, such as differential forms, optimization theory or indeed eigenvalue solutions. It transpires that optimization theory affords the most tangible approach and is the basis of the method proposed herein.

Inspection of the plots of orthogonal nets produced by the harmonic analysis of Chapter 3 indicated that each set of trajectories of the α-β net are the envelopes of a family of circles as illustrated in Fig. 5.4. By assuming that points of tangency of certain members of the infinite set of circles bounded by the mean stress contours lie on the required trajectory, the optimization problem for finding the locus of the centres reduces to the statement:

'Given two non intersecting curves in a plane find the family of circles that meets the constraint of tangency to the given curves and in addition ensures that no one member of the family intersects any other member.'

In other words the optimization problem in algebraic terms is as follows:

Minimize $C = (x_1 - h)^2 + (x_2 - k)^2$

Subject to the equalities

$$f_1(x_1) = P_1(x_1, x_2)$$
$$f_2(x_1) = P_2(x_1, x_2)$$
$$f_3(x_1) = P_3(x_1, x_2)$$

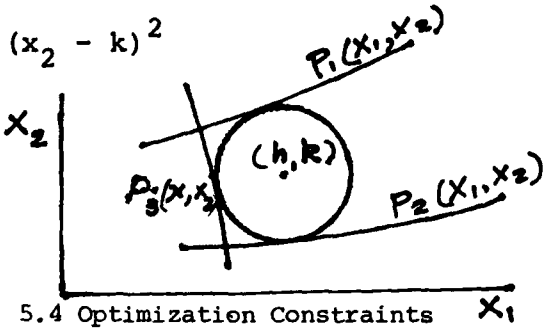

Fig. 5.4 Optimization Constraints

where the solution domain is depicted in Fig. 5.4.

Posed in this fashion the optimization problem is nonlinear and moreover the constraints are not known a priori; in particular the co-ordinates of the constraint represented by $P_3(x_1, x_2)$ depends on a previous solution step. One way of making the problem tractable is to consider one circle at a time and to use a local coordinate system suitably located on one of the fixed constraints. An algorithm to establish the centre and minimum radius which satisfies the constraints is the initial requirement. When the family of circles are defined by the co-ordinates of the points of tangency the required trajectory passes through these points. In a numerical solution it will not be necessary to graph the circles. This so-called α-β net is orthogonal but certainly is not identical to the α-β net of plastic analysis.

Consider the isolated point P_i on a mean stress contour S_i and let a local orthonormal basis be fixed in P_i such that the tangent and normal to S_i at P_i are the mutually perpendicular axes u and v as depicted in Fig. 5 (a,b).

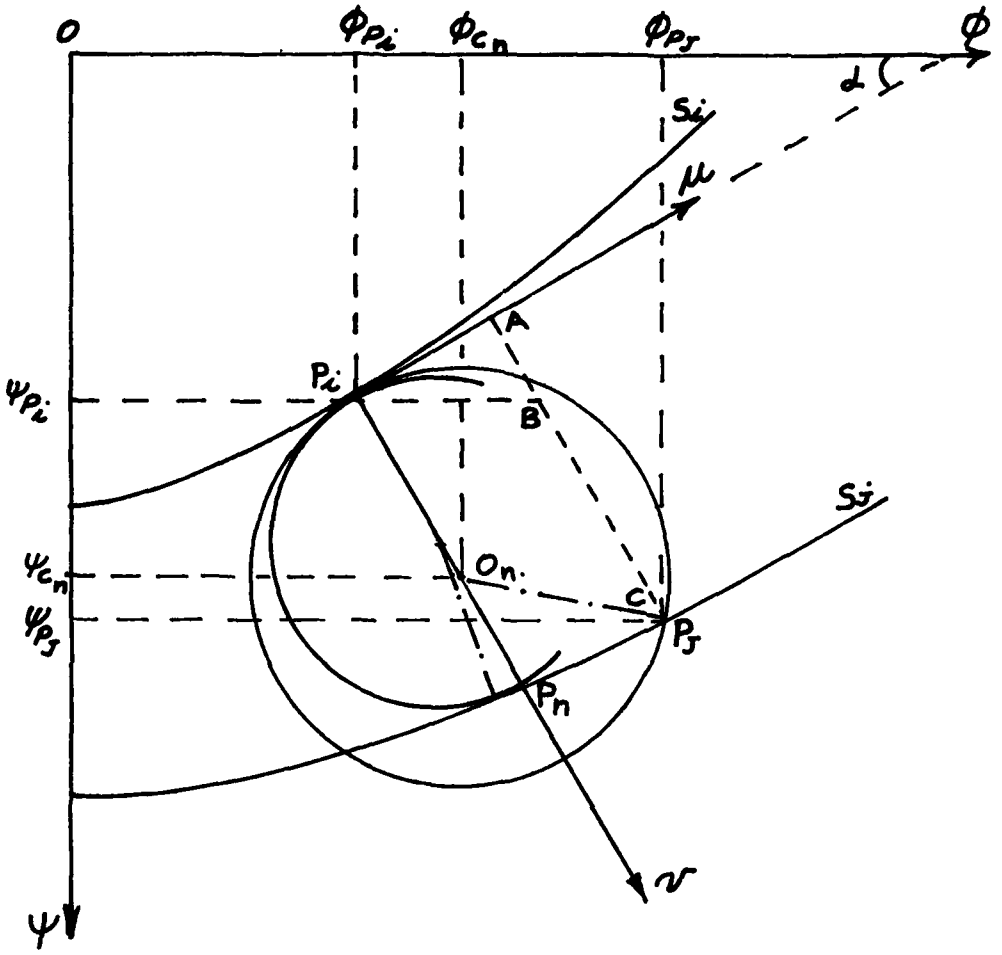

$$\bar{AC} = v_{Pj}$$

$$\bar{AB} = u_{Pj} \tan\alpha$$

$$\bar{BC} = v_{Pj} - u_{Pj} \tan\alpha$$

$$\phi_{Pj} = \phi_{Pi} + u_{Pj} \sec\alpha + (v_{Pj} - u_{Pj} \tan\alpha) \sin\alpha$$

$$\psi_{Pj} = \psi_{Pi} + (v_{Pj} - u_{Pj} \tan\alpha) \cos\alpha$$

$$\phi_{Cn} = \phi_{Pi} + \frac{u_{Pj}^2 + v_{Pj}^2}{2 v_{Pj}} \sin\alpha \qquad \psi_{Cn} = \psi_{Pi} + \frac{u_{Pj}^2 + v_{Pj}^2}{2 v_{Pj}} \cos\alpha$$

Fig. 5.5a System Coordinates : u - positive

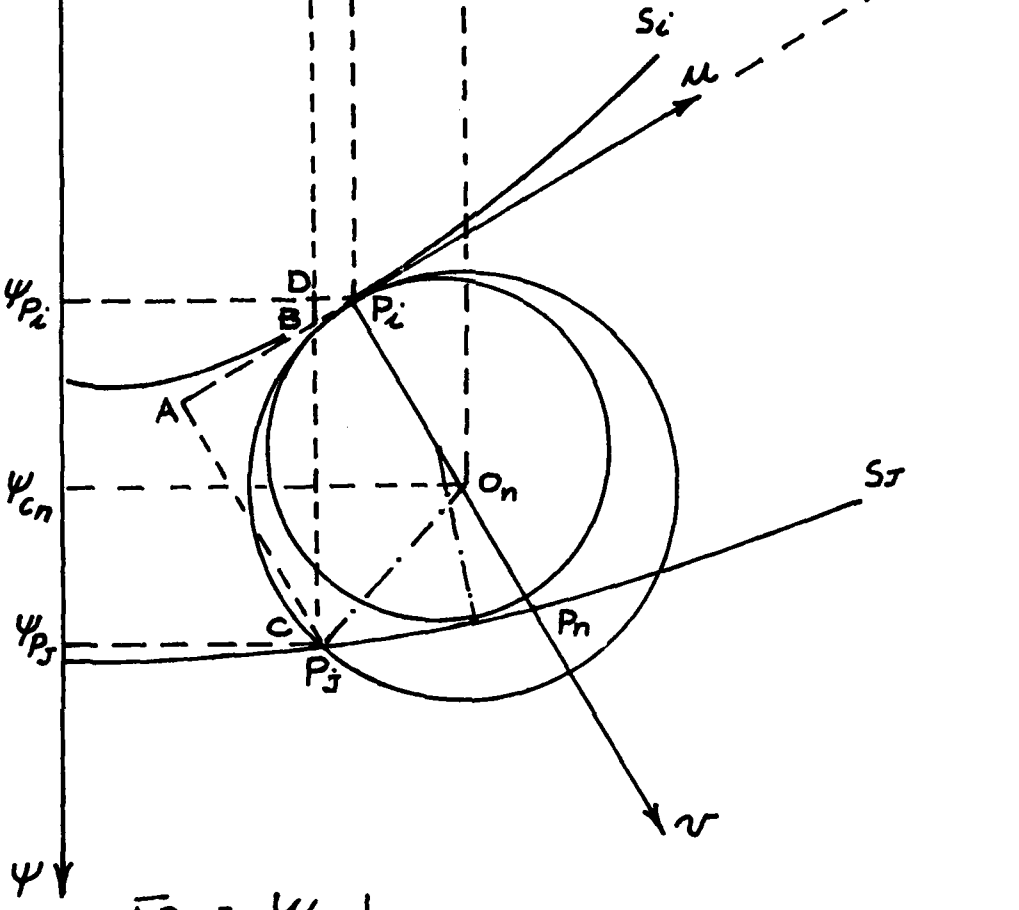

$$\overline{AP_i} = |u_{P_J}|$$

$$\overline{AB} = v_{Pj} \tan\alpha$$

$$\overline{BP_i} = u_{Pj} - v_{P_j} \tan\alpha$$

$$\overline{DP_i} = (u_{Pj} - v_{P_j} \tan\alpha)\cos\alpha$$

$$\phi_{Pj} = \phi_{Pi} - (u_{Pj} - v_{Pj} \tan\alpha)\cos\alpha$$

$$\psi_{Pj} = \psi_{Pi} + v_{Pj} \sec\alpha + (u_{Pj} - v_{P_J} \tan\alpha)\sin\alpha$$

$$\phi_{cn} = \phi_{Pi} + \frac{u_{P_J}^2 + v_{P_J}^2}{2 v_{P_J}} \sin\alpha \quad : \quad \psi_{cn} = \psi_{Pi} + \frac{u_{P_J}^2 + v_{P_J}^2}{2 v_{P_J}} \cos\alpha$$

Fig. 5.5b System Coordinates : u - negative

A neighbouring contour S_j must touch the circle which has the tangent u at P_i and centre on the normal. The circle will satisfy two of the three constraints if it touches but does not intersect the curve S_j. In order to find the centre of this inscribed circle the length of the radius must be minimised over the set of all the circles that can be drawn through P_i with a common tangent P_i as depicted in Fig. 5.5a or Fig. 5.5b. Because the set is infinite and unbounded it is necessary to confine the search to a fixed interval measured along the curve S_j. Let the interval have as end points the intersection of the normal from P_i on S_j and an arbitrary point denoted by P_j on S_j. The equation of the circles that intersect the curve S_j in the interval is given in implicit form by the expression:-

$$u^2 - 2vr + v^2 = 0 \qquad 5.16$$

and the centres are located at u_c and v_c of the local co-ordinate system where it follows from Equation 5.16.

$$u_{c_n} = 0$$

$$v_{c_n} = \frac{u_{p_j}^2 + v_{p_j}^2}{2v_{p_j}} \qquad n = 1,2,3,... \qquad 5.17$$

The circle of radius $r_n = |v_{c_n}|$ is the required member of the family when r_n is an extremum value. The minimum value is easily found by the Fibonacci search method implemented

by sampling along the curve S_j in the prescribed interval.*

The remaining constraint is satisfied by insisting that two neighbouring circles bounded by S_i and S_j have their centres separated by the sum of their respective radii taken along the curve joining the centres. To implement this constraint let the initial trial circles intersect i.e. the radical axis lies on both circles. In subsequent steps the intersection on the classical Venn-type diagram is reduced to a null set which then satisfies the third constraint.

Thus far the point P_i is arbitrarily positioned on the curve S_i. In order to locate the first trajectory to S_i we need a symmetry axis where the circle that starts the process can be defined without resort to the search technique. The radius of the initial circle in each flow tube is calculated from the intercept of S_i and S_j on the axis of symmetry. It transpires that a good first approximation to the location of P_i is given by offsetting P_i a distance of $2r_a$ along the curve S_i where r_a represents the radius of the predefined circle. The point P_j is located at a distance r_a along S_j. For either parallel or diverging curves (S_i and S_j) this choice ensures that the first trial circle intersects the previous best fit to the given constraints. The final position of P_i on

---

* The search employs the Fibonacci sequence of integer values given by:

$$F_n = \frac{\sqrt{5}}{5}\left[\left(\frac{1+\sqrt{5}}{2}\right)^n - \left(\frac{1-\sqrt{5}}{2}\right)^n\right]$$

Alternatively a tabulation of sampling stations based on this formula is available. Henley and Williams (1972).

the curve S_i is found by iteration using as incremental steps the distances Δ given by the Expression 5.18 and repeated application of the Fibonacci search,

$$\Delta = \frac{2r_{n+1}\,\delta}{r_n + r_{n+1}} \qquad 5.18$$

where δ denotes the overlap of the two circles along the curve through their centres cf. Fig. 5.6
r_n and r_{n+1} are the radii of the neighbouring circles.

If the curves S_i and S_j derive from a functional relationship such as the Eqn. 5.3, it merely remains to relate the local coordinate system to the global axes. For the sake of generality the point P_j is taken to right of the normal P_n in addition to the left of the point which is the desired location of P_j in this context as shown in Fig. 5.5.b The coordinate systems provide the relationships:

$$\phi_{P_j} = \phi_{P_i} - (u_{P_j} - v_{P_j} \tan\alpha)\cos\alpha$$

$$\Psi_{P_j} = \Psi_{P_i} + v_{P_j} \sec\alpha + (u_{P_j} - v_{P_j} \tan\alpha)\sin\alpha \qquad 5.19$$

where $\tan\alpha$ is the slope of the tangent at P_i, and (ϕ_p, Ψ_p) represent global coordinates of points on the mean stress contours. By matrix inversion the values of u_p, v_p become the dependent variables required for evaluating the radii of the inscribed circles. Of course in a computer program it is not necessary to graph the circles; the global coordinates of the points of tangency and the location of centres is all that is required from the iteration process.

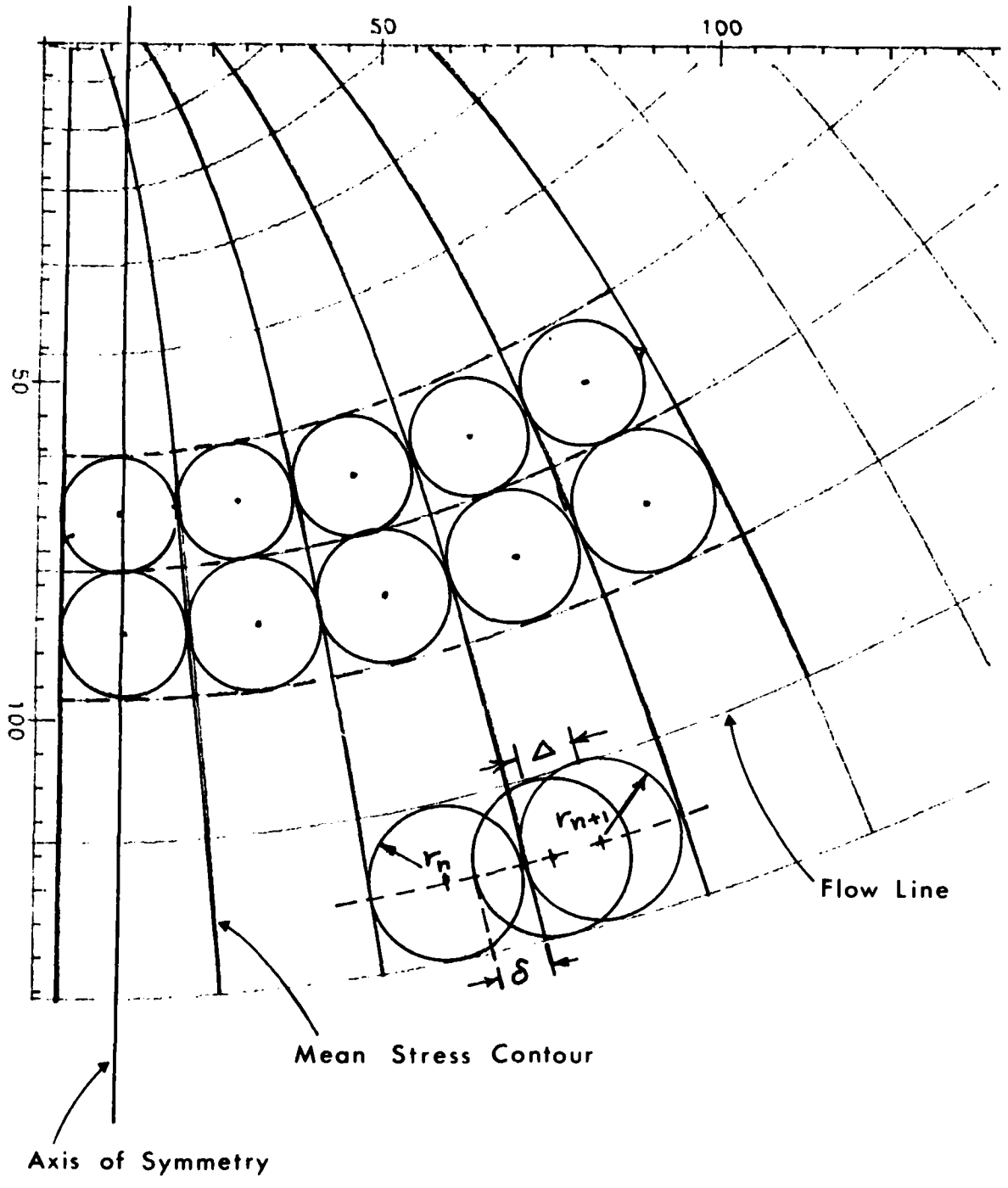

Fig. 5.6 INSCRIBED CIRCLES ON AN ORTHOGONAL NET.

The trajectories representing the flow lines pass through the contact points of the inscribed circles, hence it is necessary to generate a curve through the centres of the circles, and subsequently to find the contact points by offsetting chord lengths along the median curve equal to the sum of the radii of all feasible circles within the flow tube.

At first sight the procedure outlined above might seem complicated; in fact it is a straightforward programming exercise with only one exceptional difficulty. The difficulty forecasted is that of finding the intersection point of the normal which bounds the search level. The difficulty is exacerbated by the use of parametric cubic splines. The normal at the point $P_i(\phi_i,\Psi_i)$ is given by (cf. Fig. 5.5):

$$\Psi - \Psi_i = -(\phi - \phi_i)\cot\alpha$$

and the spline fit to S_j is of the form (Equation 4.16):

$$\phi = a_1 t^3 + b_j t^2 + c_J t + d_J$$

$$\Psi = e_J t^3 + f_J t^2 + g_J t + h_J$$

Thus, the coordinates of the intersection must be deduced by solving for the parameter t between those three equations and subsequently finding the global coordinates represented by t. Here the t-parameter is one of the roots of a cubic equation viz.

$$(a_J \cot\alpha + e_J)t^3 + (b_J \cot\alpha + f_J)t^2 + (c_J \cot\alpha + g_J)t + k = 0$$

where $k = \Psi_i + \theta_i\cot\alpha - h_J - d_J\cot\alpha$

5.20

STEP			OPERATION
1.	Loading	:	Specify boundary conditions Approximate tractions by continuous functions on boundary.
2.	Stress Distribution	:	Solve finite difference equations for Stress Components.
3.	Equi Stress Lines	:	Plot contours of selected stress component β-lines.
4.	Interpolation	:	Pass spline function through stress contours.
5.	Trajectories	:	Generate orthogonal trajectories to stress contours by search routine α-lines.
6.	Mesh Description	:	Store Cartesean coordinates of α-β intersections.
7.	Cell Dimension	:	Find cell dimensions and Jacobian transformation of areas.
8.	Data Transfer	:	Transfer data to flow Analysis Program.

5.7 Flow Chart : Numerical solution of Potential Stress Field.

Because of multiple roots of which only one is relevant, the Eqn. 5.20 can prove a nuisance in numerical solutions. Indeed, the main difficulty arises from the fact that the constants a_J, b_J etc. are specific to the knots on the spline and hence it is necessary to specify the regime of parameter t beforehand. One can only hope that this problem can be resolved by neat programming! If this drawback is removed it may even become practicable to find the coordinates of the intersection of the trajectories which is regarded as the final (but not essential) step in the proposed method. The procedure is illustrated by the flowchart in Fig. 5.7.

CHAPTER 6

FINITE ELEMENT ANALYSES OF CREEP

AND

CONTINUUM MECHANICS

6.1 *Introduction*

In this Chapter a brief review of the application of finite elements is presented as background to further development of the method in this research project. The review is mainly prepared from the formulation given by Penny and Marriott (1971); this treatment is elementary but has the appeal that it contains the fundamentals which form the basis of subsequent literature on the topic. The present author has endeavoured to concentrate on those sections that are not held in common by the various contributors (as for instance the peripheral development of solution routines for time stepping/instability caused by ill-conditioned matrices and like problems). The author's contribution centres around the manipulation of reference frames and the handling of creep test data in analyses.

6.2 *Summary of Matrix Displacement Method*

The initial loading problem is solved first; initial strains due to plasticity, creep, thermal variations are denoted by a vector $\{\varepsilon_i\}$ and the matrix algebra is in the usual notation. Superscript 'e' refers to element quantities. Subscript 'el' refers to elastic properties and subscript c to creep. Primed quantities refer to local element coordinates.

The procedure is as follows:

(a) Relate element strains $\{\varepsilon^e\}$ to element nodal displacements $\{\delta^{e'}\}$ using a convenient local set of coordinates

$$\{\varepsilon^e\} = [B]\{\delta^{e'}\}$$

(b) Relate element stresses $\{\sigma^e\}$ to element strains

$$\{\sigma^e\} = [D]\{\varepsilon_{el}\} = [D](\{\varepsilon^e\}-\{\varepsilon_1\})$$

(c) Construct element force/displacement equations in local coordinates

$$\{F^{e'}\} = [k^{e'}]\{\delta^{e'}\} \{F_1'\}$$

where $\{F^{e'}\}$ are the nodal forces

$$[k^{e'}] = \int_{vol}[B]^T [D][B] \, d(vol)$$

$$\{F_1^{e'}\} = \int_{vol}[B]^T [D]\{\varepsilon_1\} \, d(vol)$$

(d) Construct a matrix $[A]$ transforming local coordinates $\{x'\}$ to global coordinates $\{x\}$, or alternatively specify displacements in terms of shape functions referred to nodal coordinates.

(e) Solve assembled equilibrium equations for $\{\delta^e\}$ and element stresses

$$\{\sigma^e\} = [D]([B] [A^{-1}]\{\delta^e\}-\{\varepsilon_1\})$$

(f) Calculate creep rates using a creep law in terms of equivalent stress components or stress invariants

$$\{\dot{\varepsilon}_c\}^T = \{\dot{\varepsilon}_{cx}\ \dot{\varepsilon}_{cy}\ \dot{\varepsilon}_{cz}\ \dot{\alpha}_{cxy}\ \dot{\alpha}_{cxz}\ \dot{\alpha}_{czx}\}$$

where for example

$$\dot{\varepsilon}_{cx} = \frac{\overset{*}{\sigma}^{m-1}}{\overset{*}{\varepsilon}} \left(\sigma_x - \frac{\sigma_y+\sigma_z}{2}\right)$$

$$\overset{*}{\sigma} = \frac{1}{\sqrt{2}}\left[(\sigma_x-\sigma_y)^2 + (\sigma_y-\sigma_z)^2 + (\sigma_z-\sigma_x)^2 + 6(\tau_{xy}^2 + \tau_{yz}^2 + \tau_{zx}^2)\right]^{1/2}$$

$$\overset{*}{\varepsilon} = \frac{\sqrt{2}}{3}\left[(\varepsilon_x-\varepsilon_y)^2 + (\varepsilon_y-\varepsilon_z)^2 + (\varepsilon_z-\varepsilon_x)^2 + 6(\tau_{xy}^2 + \tau_{yz}^2 + \tau_{zx}^2)\right]^{1/2}$$

(g) Calculate the displacement and stress rates with replacement of all terms of the elastic analysis by their rates. In particular, for creep $\{\varepsilon_1\}$ becomes $\{\dot{\varepsilon}_c\}$

$$\{\dot{\varepsilon}^e\} = [B]\ [A^{-1}]\{\dot{\delta}^e\}$$

$$\{\dot{\sigma}^e\} = [D]([B][A^{-1}]\{\dot{\delta}^e\} - \{\dot{\varepsilon}_1\})$$

(h) Choose a small time interval $\Delta\tau$ and calculate quantities at the end of that interval e.g.

$$\{\sigma^e\}_{\tau+\Delta\tau} = \{\sigma^e\}_\tau + \{\dot{\sigma}^e\}\Delta\tau$$

(i) Repeat for successive time increments until a stationary state is achieved.

This summarizes the finite element technique if a constitutive equation is adopted to describe material behaviour.

Comment: The formulation outlined above is particularly applicable to forced flow where the stress distribution as a function of time is the main interest.

For the sake of completeness the equivalent creep stress-vs-strain relationships for a body of revolution with axial symmetry are listed as follows:

$$\Delta\varepsilon_{r,c} = \frac{\Delta\overset{*}{\varepsilon}}{\overset{*}{\sigma}}\left(\sigma_r - \frac{\sigma_\theta+\sigma_z}{2}\right)$$

$$\Delta\varepsilon_{\theta,c} = \frac{\Delta\overset{*}{\varepsilon}}{\overset{*}{\sigma}}\left(\sigma_\theta - \frac{\sigma_r+\sigma_z}{2}\right)$$

$$\Delta\varepsilon_{z,c} = -(\Delta\varepsilon_{r,c}+\varepsilon_{\sigma,c})$$

$$\Delta\gamma_{rz,c} = \frac{3}{2}\frac{\Delta\overset{*}{\varepsilon}}{\overset{*}{\sigma}}\tau_{rz}$$

where

$$\overset{*}{\sigma} = \frac{1}{\sqrt{2}}\left[(\sigma_r-\sigma_\theta)^2+(\sigma_\theta-\sigma_z)^2+(\sigma_z-\sigma_r)^2+6\tau_{rz}^2\right]^{1/2}$$

$$\Delta\overset{*}{\varepsilon} = \frac{\sqrt{2}}{3}\left[(\Delta\varepsilon_{r,c}-\Delta\varepsilon_{\theta,c})^2+(\Delta\varepsilon_{\theta,c}-\Delta\varepsilon_{z,c})^2+(\Delta\varepsilon_{z,c}-\Delta\varepsilon_{r,c})^2+6\Delta\gamma_{rz,c}^2\right]^{1/2}$$

6.3 *Discretization based on Stress Fields*

In a continuum problem the field variable, whether it be stress, displacement or some other quantity, possesses infinitely many values because it is a function of each generic point in the region. The finite element process reduces the problem to one of a finite number of unknowns at prescribed locations (element nodes) in terms of assumed approximating functions within each element. This discretization known as mesh generation is ordinarily dictated by the geometrical configuration of the solution domain and by the implementation of the boundary conditions. However, the process of discretizing the interior of the region is generally one of analytical preference; a mesh which consists of triangles (straight or curved sides) meets most applications. It has been the usual practice to attempt the simultaneous evaluation of stress and displacement in the primary analysis using elaborate finite element programs, Key et al. (1978). This approach is standard practice if the stress field is not invariant with the elapsed time of straining the material. However, for those problems where the stresses in the steady state have essentially the same magnitude as the elastic stresses the development thus far indicates that a simplistic approach is possible, which obviates the need for a finite element analysis. Once the stresses are evaluated it merely remains to introduce some form of constitutive relationship to establish the displacement field by integration.

6.4 *Incremental Solution of Displacement Field*

At the outset the stress distribution on a cell bounded by mean normal stress contours (isopacics) and flow lines was illustrated in Fig. 2.1.For the cases of plane strain and

axisymmetric problems the mean stress distributions are determinable by the method described in Chapter 5 (or indeed by the more conventional method, Airy stress functions, boundary elements (BIEM) or finite elements (FEM).

Assume that it is possible to relate the straining of the material to localised values of a function of the stresses; for instance the normal stress gradient is the function suggested in Chapter 2. On this basis the displacement field will be evaluated by using the relationships expressed in the theory of finite strain and the coordinate transformations of continuum mechanics. Herein the pertinent information follows closely the treatment of continuum mechanics to be found in texts by Sokolnikoff (1967) and Hodge (1970). For the sake of unification the author has taken some liberties with the notations in these texts, and an attempt has been made to couch the analysis in terminology familiar to readers of engineering literature.

According to Sokolinikoff the deformation of a continuum medium can best be described with respect to three reference frames as shown in Fig. 6.1; a fixed reference frame Y determined by the basis c_i; a moving reference frame ζ with basis b_i and a fixed reference frame x with basis a_i. The undeformed region is denoted by Ω_o and the same region after deformation at elapsed time t is denoted by Ω_t.
Two points P_o and P_o' will arrive at the positions P and P' in Ω_t, respectively, if the continuum is disturbed by external (or internal) tractions. The relationship between the disturbed and undisturbed positions of P_o and P_o' can be established in terms of the three coordinate systems; the Y system is Cartesian and the X - systems in general are

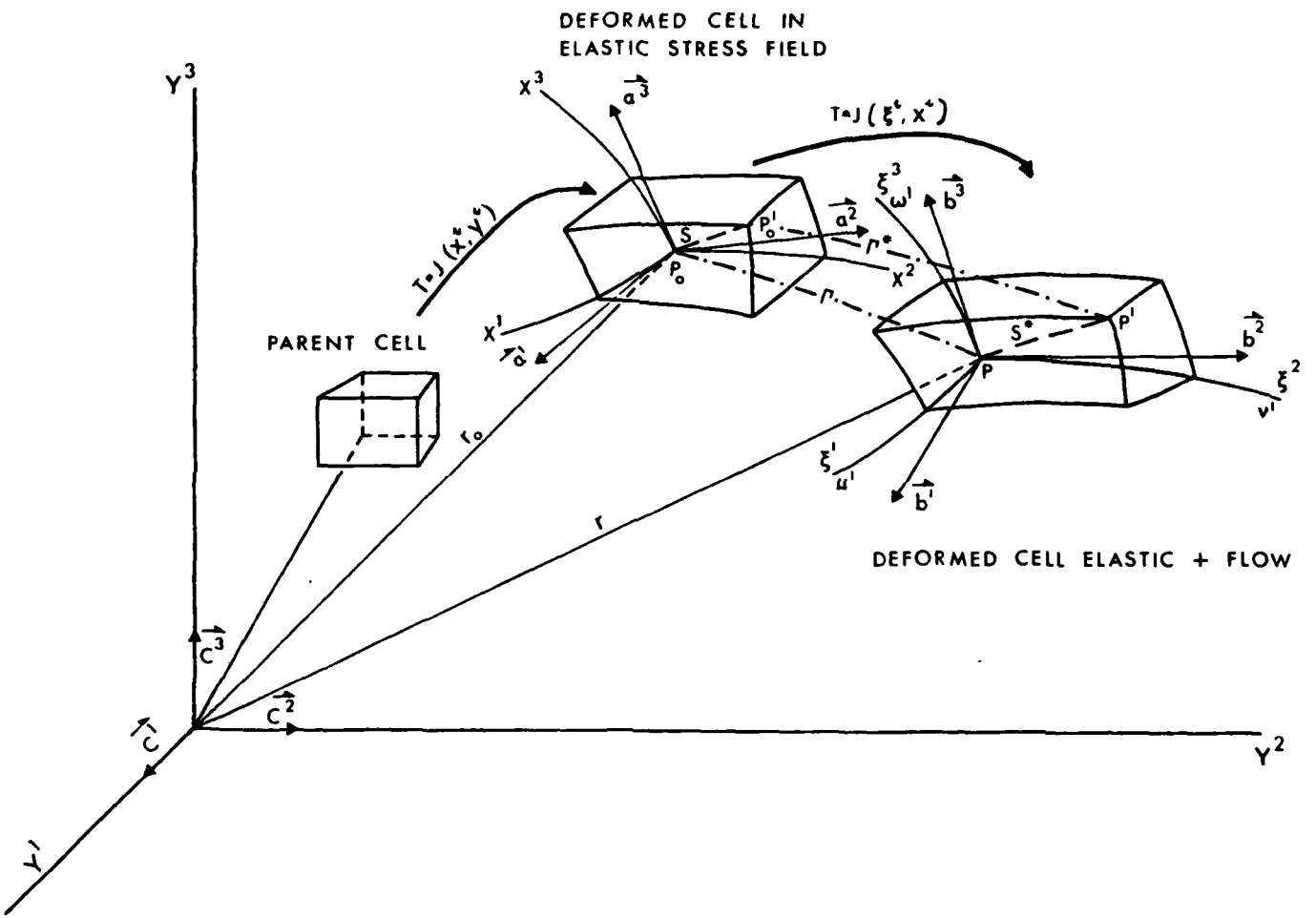

FIG 6.1. KINEMATICS OF A DEFORMABLE CONTINUUM

curvilinear.* Reference to Fig. 6.1 leads to the following:-

$$\xi_i = \xi_i(x^1, x^2, x^3, t)$$

with inverse

$$x^i = x^i(\xi^1, \xi^2, \xi^3, t)$$

A material point P_o in Ω_o relative to the orthogonal Cartesian frame Y is determined by the position vector

$$r_o = c_i y_o^i(x^1, x^2, x^3, t)$$

The location of the same point P in t is determined by the vector

$$\vec{r} = \vec{c}_i \; y^i(\xi^1, \xi^2, \xi^3, t)$$

The base vectors b_J in the moving frame ξ are given by

$$b_J = \frac{\delta r}{\delta \xi^J} = c_i \frac{\delta y^i(x,t)}{\delta \xi^J}$$

The corresponding base vectors in Ω_o are denoted by

$$a_J = \frac{\delta r_o}{\delta x^J} \quad c_i \frac{\delta y^i(x,t_o)}{\delta x^J}$$

The labels (x^1, x^2, x^3) of a given material point P_o in the X-frame and (ξ^1, ξ^2, ξ^3) in the ξ-frame have the same values and transposition of the indices is adopted for ease of writing as the occasion presents (except for base vectors for which reciprocal basis are a^i, b^i, c^i). With reference to Fig. 6.1 the following relationships can be written by inspection of the initial and final geometry.

---

* For generality the curvilinear coordinates are not necessarily orthogonal sets.

Vector $\vec{OP} = \vec{OP}_o + \vec{\Gamma}$

$$\begin{array}{ccc} \vec{P_oP_o^1} & \Rightarrow & \vec{PP^1} \\ \Downarrow & & \Downarrow \\ x_i(t_o) & & x_i(t) \\ \Downarrow & & \Downarrow \\ x_i(\text{base } a_i) & & \xi_i \ (\text{base } b_i) \end{array} \qquad i = 1, 2, 3$$

$$a_i = \frac{\delta(\vec{OP_o})}{\delta x_i} \qquad b_i = \frac{\delta(\vec{OP})}{\delta x_i}$$

$$\therefore \quad \frac{\delta(\vec{OP})}{\delta x_i} = \frac{\delta(\vec{OP_o})}{\delta x_i} + \frac{\vec{\delta\Gamma}}{\delta x_i}$$

$$\text{or} \quad b_i = a_i + \frac{\vec{\delta\Gamma}}{\delta x_i}$$

The displacement vector Γ of the point P_o is defined by

$$\vec{\Gamma} = \vec{r} - \vec{r}_o$$

and the component of Γ relative to basis a_i by (u,v,w), and its components relative to basis b_i by (u^1,v^1,w^1).

The vector $\vec{P_oP_o^1} = d\vec{r}_o$ which can be expressed in the form

$$d\vec{r}_o = a_i dx_i$$

and the square of the arc elements ds_o in Ω_o is

$$(ds_o)^2 = d\vec{r}_o \cdot d\vec{r}_o = a_I a_J dx_i dx_J$$

$$= h_{iJ} dx_i dx_J$$

where h_{iJ} denotes the metric coefficient. 6.1

Similarly the square of the element of arc ds in Ωt determined by the corresponding vector PP' can be expressed as

$$dr = b_i dx_i$$

$$\therefore (ds)^2 = b_i \cdot b_J dx_i dx_J$$

$$g_{iJ}\, dx_i\, dx_J \qquad 6.2$$

Again g_{ij} is the metric coefficient (the dot product of two vectors and is a scalar).

In expanded form this reads

$$\begin{aligned}(ds)^2 &= g_{11}(dx_1)^2 + g_{12}dx_1dx_2 + g_{13}dx_1dx_3 \\ &+ g_{21}dx_2dx_1 + g_{22}(dx_2)^2 + g_{23}dx_2dx_3 \\ &+ g_{31}dx_3dx_1 + g_{32}dx_3dx_2 + g_{33}(dx_3)^2\end{aligned}$$

or in compact quadratic form

$$(ds)^2 = \begin{bmatrix} dx_1 & dx_2 & dx_3 \end{bmatrix} \begin{bmatrix} g_{11} & g_{12} & g_{13} \\ g_{21} & g_{22} & g_{23} \\ g_{31} & g_{32} & g_{33} \end{bmatrix} \begin{Bmatrix} dx_1 \\ dx_2 \\ dx_3 \end{Bmatrix}$$

$$= (dx_i)^T (g_{iJ})\, dx_J \ ,$$

wherein

$$g_{iJ} = \sum_{k=1}^{3} \frac{\delta \xi k}{\delta x_i} \frac{\delta \xi k}{\delta x_J} \qquad i,j = 1,2,3 \qquad 6.3$$

i.e.

$$g_{11} = \left(\frac{\delta \xi_1}{\delta x_1}\right)^2 + \left(\frac{\delta \xi_2}{\delta x_1}\right)^2 + \left(\frac{\delta \xi_3}{\delta x_1}\right)^2$$

$$g_{12} = \frac{\delta \xi_1}{\delta x_1}\frac{\delta \xi_1}{\delta x_2} + \frac{\delta \xi_2}{\delta x_1}\frac{\delta \xi_2}{\delta x_2} + \frac{\delta \xi_3}{\delta x_1}\frac{\delta \xi_3}{\delta x_2}$$

6.5 *Strain Rate*

Finite strain is defined by one of the following:-

(a) Green's strain tensor
(b) Almansi's strain tensor
(c) Natural/logarithmic strain

The Green's tensor gives quadratic strains with respect to the initial coordinates by the definition:-

$$\varepsilon_{jk} = \frac{1}{2}\left(\frac{\delta \xi_i}{\delta x_J} \frac{\delta \xi_i}{\delta x_k} - \delta_{jk}\right)$$

$$= \frac{1}{2}\left[\left(\frac{ds}{ds_o}\right)^2 - 1\right] \qquad 6.4$$

where δ_{Jk} denotes the Kronecker delta and $\frac{ds}{ds_o}$ is the length ratio of the line element initially parallel to the x_1-axis which may have any current orientation.

The Almansi tensor reads:-

$$\varepsilon_{Jk} = \frac{1}{2}\left(\delta_{Jk} - \frac{\delta x_k}{\delta \xi_i} \frac{\delta x_k}{\delta \xi_j}\right) \qquad 6.5$$

Here $\left(\frac{ds}{ds_o}\right)$ is the length ratio of the element parallel to the current axis, which generally had some other orientation in the initial state.

Thus the Green's strain tensor, which is the most commonly used measure of finite strain, gives

$$(ds)^2 - (ds_o)^2 = 2\varepsilon_{iJ}\, dx_i\, dx_J \qquad 6.6$$

Since (6.6) is an invariant and $\varepsilon_{iJ} = \varepsilon_{Ji}$ the set of functions $\varepsilon_{iJ}(x,t)$ represent a tensor L with respect to a class of

admissible transformation of coordinates X, with the basis a_i covering the region Ω_o. The same set of functions $\varepsilon_{ij}(\xi,t)$ also determines a tensor E with respect to a set of transformations of coordinates determined by the basis b_i of the final state Ω. The first interpretation is termed Lagrangian; it leads to expressions for the displacement from the position x_i in the undeformed state to the deformed position ξ_i. On the other hand the second interpretation, the Eulerian system, leads to expressions for displacements that must have taken place to get to the final position ξ from the undeformed configuration x_i. The distinction between lagrangian and eulerian variables becomes negligible for small strains and rotations.

The set of differential equations for the components of the displacement when the functions ε_{iJ} are specified becomes

$$g_{iJ} - h_{iJ} = 2\varepsilon_{iJ} \quad 2\varepsilon_{iJ} \qquad 6.7$$

Therefore, from a purely geometrical standpoint, we may bring a neighbourhood of P from its initial to its final state by first translating the neighbourhood to move P_o to P, and then by rotating it so that orthogonal coordinate axes of the initial state point in the orthogonal directions of the final state, and finally deforming the neighbourhood by stretching the three axes by the ratios of the current to the initial lengths parallel to the initial axes. Hodge (1970) pp. 135-137.

Hence an arbitrary translation of a deforming element will derive from two parts represented respectively by the strain tensor $_{iJ}$ and a rotation tensor ω_{iJ}. The elements of the strain tensor are, in a convenient notation, given by

$$\epsilon_{iJ} = \begin{bmatrix} \epsilon_{11} & \epsilon_{12} & \epsilon_{13} \\ 21 & 22 & 23 \\ \epsilon_{31} & \epsilon_{32} & \epsilon_{33} \end{bmatrix} \quad ; \quad \begin{aligned} \epsilon_{iJ} &= \frac{\delta u}{\delta x_i} \, , \, \frac{\delta v}{\delta x_J} \qquad i = J \\ &= \frac{1}{2}\left(\frac{\delta u}{\delta x_J} + \frac{\delta v}{\delta x_i}\right) \quad i \neq J \end{aligned} \qquad 6.8$$

The rotation tensor is defined by

$$w_{iJ} = \begin{bmatrix} o & -w_{12} & w_{13} \\ w_{21} & o & -w_{23} \\ -w_{31} & w_{32} & o \end{bmatrix} \; ; w_{ij} = \frac{1}{2}\left(\frac{\delta u}{\delta x_J} - \frac{\delta v}{\delta x_i}\right) \qquad 6.9$$

As each line element has its own angle of rotation the entries in w_{iJ} merely gives the average rotation components of all the line segments in the elemental body; the components of w_{iJ} represent rigid body rotations, Dym and Shames (1973), Boresi(1974). Now let P_o (x_1, x_2, x_3) devote a point at which displacement u_i^o and rotation w_{iJ}^o are known in a simply connected region.

Then the displacement at any other point P is obtained by integration along a continuous curve from P_o to P. If such a line integral is to be independent of the path it follows that the strain distribution must result in an integrand which possesses the property of an exact differential Loc cit Indeed this is the criterion used in elasticity theory to set up the compatibility equations; it forms the solitary condition on the previous set of differential equations Eqn. 6.7. Recall that in Chapter 11 the issue of continuity arose in connection with strain across contiguous flow paths. With the stipulation of the exact differential the displacement of the point P becomes

$$u_i = u_i^o + \int_{P_o}^{P} \epsilon_{iJ} \, dx_J + \int_{P_o}^{P} w_{iJ} \, dx_J \qquad 6.10$$

where

$$\frac{\delta \epsilon_{ik}}{\delta x_l} - \frac{\delta \epsilon_{il}}{\delta x_k} = 0$$

$$\frac{\delta w_{ik}}{\delta x_l} - \frac{\delta w_{il}}{\delta x_k} = 0$$

For the general case of an arbitrary integration path the displacement field must be determined by integrating the rather cumbersome integrands of Eqn 6-10 with respect to non-rectilinear coordinates. Fortunately the sets of equations 6.7 and 6.10 assume quite simple forms when an orthogonal curvilinear system with origin on a flow line is chosen.* By setting a principal coordinate direction tangential to the flow-line and by making the flow line a path of integration the equation for the displacements becomes (with reference to Fig. 6.1)

$$u_{\Gamma}(t) = u_{\Gamma}^{o} + \left[\int_{o}^{\Gamma} \dot{\epsilon}_{11}(t) d\Gamma \right]_{t}^{t+\Delta t} \qquad 6.11$$

where $\dot{\epsilon}_{11}(t)$ denotes the direct strain rate component as a function of time of straining. On an axis of symmetry, or on

---

*Along a flow line the following relationships hold:

1. rotations $w_{iJ} = 0$ due to orthogonality of coordinate axes
2. metric coefficients reduce to g_{ii}, h_{ii} and the quadratic form becomes

$$(ds)^2 = g_{11}(dx_1)^2 + g_{22}(dx_2)^2 + g_{33}(dx_3)^2$$

i.e. $g_{12} = g_{21} = a_1 \cdot a_2 = 0 \qquad g_{31} = g_{13} = a_1 \cdot a_3 = 0$

3. the displacements parallel to the flow lines are sufficient to plot a flow field. Transverse component perpendicular to flow line is determinate by property of exact differential if required.

a rigid boundary u_Γ^o is zero; the value of u_Γ represents the extension, or contraction, of a flow path relative to its length at time t measured from a fixed datum, i.e. a symmetry axis or rigid boundary.

Where the boundary itself is subject to displacements of interest, as beneath a surface traction, the Equation 6.11 provides a relationship for incremental solution of the points of the flow line with respect to the initial position. The displacements at points along the flow line are further governed by the Equation 2.10 and 2.11. (There is a direct analogy here with the problem of a non-uniform variation of temperature in a heated elastic solid; the strains at any point is given by $\varepsilon = \alpha T$ and these must be integrated with respect to the coordinates to arrive at the displacements).

Evidently the evaluation of the displacements along individual flow lines will yield the complete displacement field for axially symmetric and plane strain problems. The displacements so determined over incremental time steps, assuming a linear variation over the duration of each time step, will sum to the total displacements at any desired time t; i.e. the motion between x_n^i and x_{n-1}^i is linear. As a consequence, the incremental velocity given by $v_{n+\frac{1}{2}}^i = \Delta x^i/\Delta t$ is constant over the time increment. The author predicts that the application of Eqn. 6.11 will give an enhanced insight into flow mechanisms compared with solutions by the finite element or kernel methods discussed earlier in this report.

CHAPTER 7

INTERPRETATION OF CREEP TESTS AND SUMMARY OF INVESTIGATION

7.1 *The Theory of Creep Potential as an aid to Interpretation of Experimental Data.*

The theory of creep potential is based on concepts introduced in plasticity theory for the purpose of evaluating relative strain rates in ideal plastic solids. The plastic potential function $f(\sigma_{iJ})$ is a scalar function of stress which yields relative strain rates (the time variable is a dummy term) according to the expression Drucker and Prager (1952)

$$\dot{\varepsilon}_{iJ} = \lambda \frac{\delta f(\sigma_{iJ})}{\delta \sigma_i} \qquad 7.1$$

where λ is a non negative constant. Extension of this concept to creep leads to an analogous relationship, Penny and Marriott (1971).

$$d\varepsilon_{iJ,c} = \frac{\delta \psi}{\delta \sigma_{iJ}} d\lambda \qquad 7.2$$

For isotropic materials the experimental evidence seems to favour the von Mises criterion for formulation of creep potential surfaces. In the case of isotropic multiaxial creep the creep potential deduced from the criterion is

$$\psi(\sigma_{iJ}) = \frac{\sigma^{*2}}{3}$$

Then the creep strain increments are related to the stress components in the expression, loc cit.

$$d\varepsilon_{ij,c} = \frac{3}{2} \frac{d\bar{\varepsilon}^{*}}{\bar{\sigma}^{*}} S_{ij} \qquad 7.3$$

where $S_{ij} = \delta\psi/\delta\sigma_{ij}$ is termed the stress deviator. A similar interpretation is employed in visco-plasticity theory of Chapter I of this report. However, the application of creep potential theory has not been extensive compared with the hereditary integral theory or with the empirical constitutive relationship approach.

The present author suggests that the concept of creep potential deserves more attention than hitherto found in the literature. It is one approach that promises to inject some unification into the handling of experimental data. In order to generalise, it is imperative that different stress states can be taken into account and that no matter what is the stress state in the material the interpretation of experimental data leads to a unique value of the velocity at each point in the body. To fix ideas consider the types of data derived from the following set of laboratory tests:

1. uniaxial tension or compression on prismatic specimens
2. triaxial compression test on cylindrical specimens
3. hollow cylinder subjected to differential lateral pressures

In uniaxial tension there is no variation in stress normal to direction of flow hence the notion of creep dependence on stress gradient is inapplicable. Similarly, in the triaxial test the stress gradient between the symmetry axis and boundary is not significant as demonstrated by finite element analysis; the axial stress is virtually constant over the length of the specimen and radial and hoop stresses attain approximately 0.005 per cent. of the axial component.

A state of pure shear implies that normal stresses do not exist on the planes of maximum shear stress. On the other hand the hollow cylinder test exhibits creep under the action of stress gradient in the radial direction but the sum of the radial and hoop stresses is a constant value. In the light of the earlier discussion of stress state in the axisymmetric flow of a semi-infinite medium caused by normal stresses on a part of the boundary the hypothesis of normal stress gradient as the primary source of the forcing function appears to present just one further option for interpreting test data. The problem is how to assimilate the results of different test configurations in a unified presentation. The earlier mentioned use of effective stress-strain is one such attempt at unification as indeed the choice of constants makes the components consistent for uniaxial and multiaxial tests.*

Again the stress components octohedral normal (σ_{oct}) and octohedral shear (τ_{oct}) play a similar role as these stress components are related to the stress invariants and give a measure of the hydrostatic and the deviatoric components of the state of stress at a point. These relations are

$$\sigma_{oct} = \frac{\sigma_1 + \sigma_2 + \sigma_3}{3}$$

$$\tau_{oct} = \frac{1}{3}\{(\sigma_1 - \sigma_2)^2 + (\sigma_2 - \sigma_3)^2 + (\sigma_3 - \sigma_1)^2\}^{1/2}$$

---

* Effective stress in this context is not to be confused with the meaning of the word in Soil Mechanics literature; perhaps the term 'equivalent stress' or 'generalised stress' would avoid the ambiguity.

$$\tau_{oct} \equiv \frac{\sqrt{2}}{3}(J_1^2 - 3J_2)^{1/2}$$

$$\varepsilon_{oct} = \frac{\varepsilon_1 + \varepsilon_2 + \varepsilon_3}{3}$$

$$\gamma_{oct} = \frac{2}{3}\left[(\varepsilon_1 - \varepsilon_2)^2 + (\varepsilon_2 - \varepsilon_3)^2 + (\varepsilon_3 - \varepsilon_1)^2\right]^{1/2} \qquad 7.4$$

The spatial derivative of σ_{oct} is taken as a measure of the shearing intensity in a discretized zone according to the foregoing hypothesis of normal stress gradient as the forcing function. The hypotheses is merely a restatement of the case for creep that the von Mises criterion in plasticity theory may be extended to include dependence on hydrostatic stress. The yield surface will generate a circular cone symmetrical about the hydrostatic axis. The extended von Mises criterion takes the form, Harr (1966) pp 169

$$(\sigma_1 - \sigma_2)^2 + (\sigma_2 - \sigma_1)^2 + (\sigma_1 - \sigma_3)^2 = k(\sigma_1 + \sigma_2 + \sigma_3)^2 \qquad 7.5$$

where k is a function of frictional resistance characterised by the angle ϕ in granular media. The extended von Mises criterion is treated in more detail by Nadai (Vol. 1 pp 226-228).

Stress Manifolds

From the foregoing discussion it follows that we seek a set of functions in an n-dimensional stress space which has the property of C^1-continuity (at least in the domain of interest). Mathematically the entity of the set is termed a real analytic manifold; by definition it consists of n functions of n variables which can be expanded in a

convergent Taylor series in a neighbourhood of each point, Bruhat et al. (1977) pp 112. To be of value in the context of integration for displacement fields the tangent planes to the manifold must give the strain rate in the direction of maximum velocity; ideally the dip of the tangent plane yields the maximum strain rate. The interpretation of test data may thusly be reduced to forming the Sobolev space of functions written symbolically as

$$W_p^m(U) = F_n(\sigma_{ij}, \sigma'_{ij}, \sigma'_{ij}, \ldots) , \quad n=1,2,3,\ldots \qquad 7.6$$

Some applications of this rather advanced topic in functional analysis is covered in the Prentice-Hall Civil Engineering and Engineering Mechanics series, Oden 1979. Suffice it to say that the theory of topological spaces provides a formalised approach to characterising a set of functions and to investigating distributional partial derivatives of the set.

7.2 *Summary*

The study of creep undertaken in this report has examined the subject from a variety of standpoints. The first chapter deals with the classical theories and serves as background to further development. As with works of an original nature the outcome consists of a mixture of disappointments and satisfaction. On the negative side the postulate of a transform for quantifying strain rate is defective in the sense that the answer depends on the discretization of the solution domain, cf. Chapter 11. Another disappointing aspect emerges in Chapter 111 wherein it is shown that only a limited set of flow patterns could be generated by the proposed harmonic analysis; the set

contains few patterns symmetric about the axis of symmetry of a loaded area on a semi-infinite half space. Apart from these findings positive contributions may be claimed as follows:

1. A framework is established for predicting the displacement field as a function of time of straining provided that strain rates can be specified at sufficient points in the solution domain.

2. The stress fields are determined by a summation process in a simple algorithm.

3. The geometry of Laplacian flow nets is treated in detail as are the different types of boundary condition.

4. Computer programs have been prepared for implementing some of the analytical techniques.

5. The study culminates in the suggestion that functional analysis offers an approach to a unified interpretation of experimental data.

6. The main simplification results from the proposed method of direct integration along flow paths. This innovation allows a free choice of the strain rate tensor because infinitesimal and finite strains can be handled with equal ease in evaluating the line integral for displacement; the strain rates are formulated as a part of the interpretation of experimental data with no further implications in the analytical technique.

REFERENCES

Adeyeri, J.B. and Krizek, R.J., "Mimic Source Approach to Viscoelastic Analysis". Proc. ASCE Sym Application of Finite Element Methods in Civil Engineering, Vanderbilt University, 1969.

Ahlvin, R and Ulery, H.H., "Tabulated Vlaues for Determining the Complete Pattern of Stresses, Strains and Deflections beneath a Uniform Load on a Homogeneous Half-space". H.R.B. Bull 342, 1962.

Al Salihi, M.Z., Parametric Surfaces in Finite Element Analysis of Thin Shells. Ph.D. dissertation, University of Dublin, 1978.

Arutyunyan, N.Kh., Some Problems in the Theory of Creep in Concrete Structures. Pergamon Press, 1966.

Boresi, A.P. and Lynn, P.P., Elasticity in Engineering Mechanics, Prentice Hall, 1974.

Centurioni, L. and Viviani, A., "Contribution to Numerical Computation of Laplacian Fields". Proc. I.E.E. Vol. 122 No 11 1975.

Courant, R. and Fritz John, Calculus and Analysis Vol II.

Chang Lu, P., Introduction to Mechanics of Viscous Fluids, Holt-Reinhart, Winston, 1973.

Choquet-Bruchat, Y. Witt Morette, C.D. and Dillard-Bleick, M., Analysis Manifolds and Physics, 1977.

Dewhurst, P. and Collins, I.F., "A Matrix Technique for Constructing Slip-line Field Solutions to a Class of Plane Strain Plasticity Problems". Int. Jour. for Numerical Methods in Engineering Vol. 7, 1973.

Drucker, D.C. and Prager, W., "Soil Mechanics and Plastic Analysis or Limit Design". Quart. Appl. Math. Vol 10 No 2, 1952.

Dym, C.L. and Shames, I.H., Solid Mechanics - A Variational Approach. McGraw Hill, 1973.

Fenner, R.T., Finite Element Methods for Engineers, Macmillan, 1975.

Ford, H. and Alexander, I.M., Advanced Mechanics of Materials 2nd. Ed. Ellis Horwood, 1976.

Frind, E.O., "An Isoparametric Hermitian Finite Element for the Solution of Field Problems". Int. Jour. for Numerical Methods in Engineering No 11, 1977.

Glen Murphy, Similitude in Engineering, Ronald Press Co. 1950.

Harr, M.E., Foundations of Theoretical Soil Mechanics, McGraw Hill, 1966.

Henley, E.J. and Williams, R.A., Graph Theory in Modern Engineering. Edited by R. Bellman, University of Southern California, Academic Press, 1972.

Hildebrand, F.B., Advanced Calculus for Engineers. Prentice - Hall Inc. 1957.

Hodge, P.G. Continuum Mechanics. McGraw Hill, 1970.

Huebner, K.H., Finite Element Methods for Engineers. Wiley, 1975.

Jumikis, A.F., Introduction to Theoretical Soil Mechanics. Van Nostrand, 1967.

Key, S.W., Beisinger, Z.E. and Kreig, R.D. HONDO-11 A Finite Element Computer Program for the Large Deformation Dynamic Response of Axisymmetric Solids. Sandia National Laboratories, 1978.

Kuske, A. and Robertson, G. Photoelastic Stress Analysis. Wiley Interscience, 1974.

Marsden, J.E., and Tromba, A.J., Vector Calculus. Freeman, 1975.

Mc Conologue, D.J., "A Quasi Intrensic Scheme for passing a Smooth Curve through a Discrete set of POints". Computer Jour, No 13, 1970.

O'Laoide, B.O., Application of Potential Fields in Stress Analysis, M.Sc. dissertation, University of Dublin, 1979.

Oden, J.T., Applied Functional Analysis. Prentice-Hall Inc. 1979.

Penny, R.K. and Marriott, D.L., Design for Creep. McGraw Hill 1971.

Rabotnov, Y.N. Some Problems of the Theory of Creep. 1953.

Sampine, X., and Allen, Y., Numerical Computing. W.B.Sanders Co., 1973.

Shaug, J.G., and Bruch, J.C., "Seepage through a Homogeneous Dam , Second Int. Sym. Finite Elements in Flow Problems". ICCAD Santa Margherita Ligure Italy, 1976.

Sokolinikoff, I.S., Tensor Analysis. Wiley, 1964.

Thrower, E.N., "Methods for Predicting Deformation in Road Pavements". Fourth Int. Conf. on the Structural Design of Aspahlt Pavements Vol 1 Ann Arbor, 1977.

Timoshanko, S. and Goodier, J.N., Theory of Elasticity, McGraw Hill, 1951.

Unksov, E.P., An Engineering Theory of Plasticity. Butterworths, 1961.

Zienkiewicz, O.C. and Godbole, P.N., "Viscous Incompressible Flow with Special Reference to Non-Newtonian Flow". Finite Element in Fluids, Vol I, Wiley, 1975.

BIBLIOGRAPHY

Christian, J.T. and Watt, B.J., "Viscoelastic Analysis of Soil Deformation" Proc. Sym. Applications of the Finite Element Method in Geotechnical Engineering, Vicksburg, Miss, 1972.

England, G.L., "The Direct Calculation of Stresses in Creeping Concrete and Concrete Structures. Proc. Sym. Stress Analysis, University of Southampton, 1969. *

Hu, S.T., Differential Manifolds. Holt Reinhart and Winston, 1969.

Leckie, F.A., "Structural Theorems of Creep and their implications". Loc. cit. *

McConnell, A.J., Application of Tensor Analysis. Dover Press 1957.

Nadia, A. Theory of Flow and Fracture of Solids. Vols 1 and 2 McGraw Hill, 1963.

Paramichael, N and Whitman, J.R. "Cubic Spline Interpolation of Harmonic Functions" B.I.T., Bind 14, Heffe NR4, 1974.

Sokolnikoff, I.S. and Redheffer, R.M. Mathematics and Physics of Modern Engineering. McGraw Hill,1966.

UNCLASSIFIED

R&D 2287-EN

SECURITY CLASSIFICATION OF THIS PAGE (When Data Entered)

REPORT DOCUMENTATION PAGE	READ INSTRUCTIONS BEFORE COMPLETING FORM
1. REPORT NUMBER	2. GOVT ACCESSION NO. AD-A118 224	3. RECIPIENT'S CATALOG NUMBER
4. TITLE (and Subtitle) Numerical Methods for Creep Analysis in Geotechnical Problems.	5. TYPE OF REPORT & PERIOD COVERED Final Technical Report Aug 76 - Dec 81
	6. PERFORMING ORG. REPORT NUMBER
7. AUTHOR(s) T. E. Glynn	8. CONTRACT OR GRANT NUMBER(s) DAERO-76-G-063
9. PERFORMING ORGANIZATION NAME AND ADDRESS School of Engineering University of Dublin Trinity College Dublin, Ireland	10. PROGRAM ELEMENT, PROJECT, TASK AREA & WORK UNIT NUMBERS 61102A IT161102BH57-01
11. CONTROLLING OFFICE NAME AND ADDRESS USA Research, Development & Standardization Group - UK Box 65, FPO NY 09510	12. REPORT DATE Dec 1981
	13. NUMBER OF PAGES
14. MONITORING AGENCY NAME & ADDRESS(if different from Controlling Office)	15. SECURITY CLASS. (of this report) UNCLASSIFIED
	15a. DECLASSIFICATION/DOWNGRADING SCHEDULE

16. DISTRIBUTION STATEMENT (of this Report)

Approved for public release; distribution unlimited

17. DISTRIBUTION STATEMENT (of the abstract entered in Block 20, if different from Report)

18. SUPPLEMENTARY NOTES

19. KEY WORDS (Continue on reverse side if necessary and identify by block number)

Geotechnical Problems; Creep; Similitude; Mapping Functions; Potential Fields; Finite Elements; Contour Integrals; Functional Analysis.

20. ABSTRACT (Continue on reverse side if necessary and identify by block number)

The study of creep undertaken in this report has examined the subject from a variety of standpoints. The first chapter deals with the classical theories and serves as background to further development. As with works of an original nature the outcome consists of a mixture of disappointments and satisfaction. On the negative side the postulate of a transform for quantifying strain rate is defective in the sense that the answer depends on the discretization of the solution domain, cf. Chapter 11. Another disappointing aspect emerges in Chapter III wherein it is shown that only a

DD FORM 1 JAN 73 1473 EDITION OF 1 NOV 65 IS OBSOLETE S/N 0102-LF-014-6601

UNCLASSIFIED

SECURITY CLASSIFICATION OF THIS PAGE (When Data Entered)

20../Cont.

limited set of flow patterns could be generated by the proposed harmonic analysis; the set contains few patterns symmetric about the axis of symmetry of a loaded area on a semi-infinite half space. Apart from these findings positive contributions may be claimed as follows:

1. A framework is established for predicting the displacement field as a function of time of straining provided that strain rates can be specified at sufficient points in the solution domain.

2. The stress fields are determined by a summation process in a simple algorithm.

3. The geometry of Laplacian flow nets is treated in detail as are the different types of boundary condition.

4. Computer programs have been prepared for implementing some of the analytical techniques.

5. The study culminates in the suggestion that functional analysis offers an approach to a unified interpretation of experimental data.

6. The main simplification results from the proposed method of direct integration along flow paths. This innovation allows a free choice of the strain rate tensor because infinitesimal and finite strains can be handled with equal ease in evaluating the line integral for displacement; the strain rates are formulated as a part of the interpretation of experimental data with no further implications in the analytical technique.